MATHEMATICAL BIOSCIENCES
AND ENGINEERING
Volume **11**, Number **4**, August **2014**

doi:10.3934/mbe.2014.11.841

pp. **841–875**

EFFECTS OF NUTRIENT ENRICHMENT ON COEVOLUTION OF A STOICHIOMETRIC PRODUCER-GRAZER SYSTEM

Lina Hao, Meng Fan and Xin Wang

School of Mathematics and Statistics, Northeast Normal University
5268 Renmin Street, Changchun, Jilin, 130024, China

(Communicated by Yang Kuang)

Abstract. A simple producer-grazer model based on adaptive evolution and ecological stoichiometry is proposed and well explored to examine the patterns and consequences of adaptive changes for the evolutionary trait (i.e., body size), and also to investigate the effect of nutrient enrichment on the coevolutin of the producer and the grazer. The analytical and numerical results indicate that this simple model predicts a wide range of evolutionary dynamics and that the total nutrient concentration in the ecosystem plays a pivotal role in determining the outcome of producer-grazer coevolution. Nutrient enrichment may yield evolutionary branching, trait cycles or sensitive dependence on the initial values, depending on how much nutrient is present in the ecosystem. In the absence of grazing, the lower nutrient density facilitates the continuously stable strategy while the higher nutrient density induces evolutionary branching. When the grazer is present, with the increasing of nutrient level, the evolutionary dynamics is very complicated. The evolutionary dynamics sequentially undergo continuously stable strategy, evolutionary branching, evolutionary cycle, and sensitive dependence on the initial values. Nutrient enrichment asserts not only stabilizing but also destabilizing impact on the evolutionary dynamics. The evolutionary dynamics potentially show the paradox of nutrient enrichment. This study well documents the interplay and co-effect of the ecological and evolutionary processes.

1. **Introduction.** Evolution is the change in genetic composition of a population over successive generations, which results in the change of corresponding genotype frequencies within populations or species during the interaction of individuals with one another and with the environment [19]. Although population dynamics and evolutionary dynamics are often treated as separate fields that require different approaches and methodologies, genetic variation among individuals can have strong effects on the observed community-level dynamics. Many studies have documented that the rapid evolutionary change affects the interspecific interactions and genotypic structure and then alters ecological functions [19, 45]. Evolutionary and ecological dynamics are likely to be co-dependent when changes in genotype frequency result in a change in the phenotypic traits, which crucially affect interaction strength among populations.

2010 *Mathematics Subject Classification.* Primary: 92D25, 92D15; Secondary: 34C60, 92B05.

Key words and phrases. Co-evolution, adaptive dynamics, nutrient enrichment, ecological stoichiometry.

Supported by NSFC (No. 11271065, 10971022) and RFDP (No. 20130043110001).

Meng Fan is the corresponding author.

Although the impact of ecological changes on evolutionary responses has long been acknowledged, the converse has been predominantly neglected, particularly empirically [15]. Population growth is a consequence of multiple processes, which strengthen arguments advocating integrated approaches to assess how populations respond to the environments. Both the evolution and the population biology must be integrated together in natural communities [18, 19, 24, 47]. One of the central issues of evolutionary dynamics is to characterize the evolutionary process at community levels such as continuously stable strategy, evolutionary branching, evolutionary cycle et al.

In term of methodology, there are several different approaches to modeling evolutionary changes in dynamical models of ecological communities. One is the locus-based population genetic models [36], which directly incorporate basic population genetics into population dynamics. As an alternative, quantitative trait (QT) models [18] describe the evolutionary change of a phenotypic trait under selection and affecting the population dynamics. Adaptive dynamics (AD) is another approach to studying the evolutionary phenotypic changes in evolving populations when fitness is density or frequency dependent [21], which assumes that evolutionary and ecological dynamics occur on different time-scales and separate the two dynamical processes analytically, draws on the feedback between ecological and evolutionary processes, and has been proved to be a useful framework to model the evolution of quantitative traits. AD models have been and continue to be a useful method of attacking a number of interesting and important issues in evolution and related subjects such as long-term phenotypic evolution under complex ecological scenarios in the terms of maintenance of genetic variation, coevolution or sympatric speciation [20, 44].

Nutrient limitation determines the primary production and species composition of many aquatic and terrestrial ecosystems. Nutrient enrichment becomes particularly relevant as human activities profoundly enrich the biosphere with three elements that are most critical to all life- C, N, and P (via rising CO_2, anthropogenic N fixation, and mining of phosphates for fertilizers). Nutrient enrichment from human activities represents one of the greatest threats to global ecosystems with significant consequences for ecosystem structure and function [8], but its effects on ecosystem productivity can differ greatly. In aquatic ecosystems, the nutrients are of paramount importance for primary production and the important role played by nutrients in lake problems is generally accepted today [3]. Mounting evidences indicate that nutrients assert profound impacts not only on the ecological dynamics by bottom up control [1, 4, 8, 12] but also on the evolution dynamics [19, 22, 23, 30, 28, 32].

In mathematical modeling, one typical and reasonable approach to incorporating the nutrient (i.e., phosphorus) into the model is based on the principles of ecological stoichiometry. The theory of ecological stoichiometry [40], which refers to the balance of energy and multiple chemical substances in living systems, has seen some exciting progresses in modeling and understanding ecosystems [11, 31, 35, 40, 41, 43]. Ecological stoichiometry provides rigorous and ubiquitous mechanistic basis for exploring the effect of nutrients on the evolutionary dynamics because the evolutionary model is generally determined by the fitness gradients of the ecological model. Some attempts have been made to examine the effects of the evolution of some traits relating to stoichiometry on the evolutionary dynamics [2, 5, 17, 26, 42]. However, most of those studies are just case-related or based on numerical or computational

TABLE 1. Symbols of the Model Parameters

Para.	Definition	Value	Unit	Reference
r_0	Producer's maximum growth rate with $x_1 = x_0$	1	day^{-1}	[43]
P_T	Total phosphorus	0.02	mg P/l	[31]
q_0	Producer minimal P/C	0.0038	mg P/mg C	[31]
q_2	Grazer constant P/C	0.03	mg P/mg C	[31]
c_0	Maximum strength of intraspecific competition	0.1	$(\text{day}\cdot\text{mg C/l})^{-1}$	Default
d_1	Loss rate of producer	0.2	day^{-1}	[11]
a_0	Maximum capture rate	0.8	$(\text{day}\cdot\text{mgC/l})^{-1}$	[11, 31]
$\hat{e}$	Maximal conversion rate of grazer	0.8		[11, 31]
d_2	Loss rate of grazer	0.2	day^{-1}	[11, 31]
x_0	Intermediate body size at which the best advantage occurs	0.5		[48]
σ_r^2	Variance of the phenotypic effect of individuals with trait x_1	0.014		[48]
σ_c^2	Variance of the phenotypic effect of individuals with traits y_1 and x_1 interactions	0.01		Default
σ_a^2	Variance of phenotypic effect of individuals with traits x_1 and x_2 interactions	0.009		Default
μ_1	Probabilities that the birth events are mutant for producer	0.1		[48]
μ_2	Probabilities that the birth events are mutant for grazer	0.1		[48]
σ_1^2	Variances of the mutation distribution of producer	0.1		[48]
σ_2^2	Variances of the mutation distribution of grazer	0.01		[48]

approach. In addition, there are less theoretical studies on identifying the effects of nutrients incorporating ecological stoichiometry on the long-term evolutionary dynamics in natural ecosystems although the coevolution dynamics of community have attracted a lot of attentions.

Motivated by the above considerations, by integrating the evolutionary dynamics with the stoichiometric theory, here we present and analyze an evolutionary stoichiometric producer-grazer (ESPG) model, which combines adaptive dynamics and ecological stoichiometry, to explore the patterns and consequences of the evolution of evolutionary trait (i.e., body size), and to expound the impacts of nutrient on the evolutionary dynamics. In Section 2, both the ecological stoichiometric model and the evolutionary model are introduced and their qualitative dynamics are mathematically explored. Section 3 deals with the evolutionary dynamics of producer when the grazer is absent. Section 4 devotes to investigating the effects of nutrient on the coevolution dynamics of the ESPG when grazer is present. Section 5 ends the paper with a discussion. To our knowledge, this is the first theoretical study on producer-grazer coevolution incorporating elements of ecological stoichiometry and adaptive dynamics and therefore constitutes a relevant contribution to integrate these two emerging frameworks.

2. **The model.** In this section, a stoichiometric producer-grazer ecological model is proposed to illustrate the effects of the total phosphorus density on the dynamics of the ecological model by qualitative analysis. Then, an evolutionary model is built based on the ecological model by applying the adaptive dynamics theory[9, 19]. Consider body sizes as the evolutionary traits and assume the pace of the change of the traits is slower than the ecological dynamics. Hence, the ecological process and the evolutionary process occur on different time-scales and can be separated analytically later.

2.1. **The ecological model.** Consider a simple community, with one limiting nutrient (say phosphorus), a primary producer ($A(t)$ (mg C/l), the density of producer at time t), and a grazer ($G(t)$ (mg C/l), the density of grazer at time t). We assume that the growth rate of primary producer is nutrient limited. As in [31], assume that the system is closed for phosphorus with a total of P_T (mg P/l) and all phosphorus in the system is divided into two pools: phosphorus in the producer and phosphorus in the grazer. Essentially, it is assumed that the free phosphorus is immediately taken by the producer. Moreover, the intracellular nutrient content (also known as cell quota) of producer (q_1 (mg P/ mg C)) varies (e.g., increases due to nutrient uptake and declines due to dilution by growth) but never falls below the minimum q_0. The cell quota of the grazer (q_2 (mg P/ mg C)) is assumed to stay constant [31, 40]. From the above assumptions, it follows that

$$P_T = q_1 A(t) + q_2 G(t).$$

In the absence of grazer, the growth of producer follows the Droop equation ([14])

$$\frac{dA}{dt} = r(1 - \frac{q_0}{q_1})A - cA^2 - d_1 A,$$

where r (day^{-1}) is the per capita maximum growth rate of producer, q_0 (mg P/mg C) is the fixed minimum cell quota of producer, c ($(day \cdot mgC/l)^{-1}$) is the intraspecific competition coefficient of producer, which is caused by non-phosphorus-dependent factors such as light, allelopathy or other nutrients et al., and d_1 (day^{-1}) is the loss rate of producer.

The grazer follows exponential decay $dG/dt = -d_2 G$ when there is no producer, where d_2 (day^{-1}) is its loss rate. Since the grazer keeps the constant cell quota for phosphorus, its growth rate can be limited not only by food quantity (producer biomass measured in carbon terms) but also by food quality (the phosphorus content in the producer, q_1). When $q_1 < q_2$, the grazer is limited by food quality and, hence, cannot incorporate the excess of carbon in the ingested food into its own biomass. Instead, the grazer respires (as CO_2), excretes or egests the excess of carbon, thus reducing its conversion efficiency. As in [31], we assume that the grazer's conversion efficiency is governed by the mass balance law: e follows a minimum function, i.e., $\hat{e}\min\{1, (P_T - q_2 G)/(q_2 A)\}$, where $\hat{e}$ is the grazer's maximal conversion efficiency achieved at good food quality (i.e. when $q_1 \geq q_2$). For simplification, the functional response of grazer is assumed to be of bilinear type, i.e., aAG, where a ($(day \cdot mgC/l)^{-1}$) is the predation rate of grazer.

Now, the stoichiometric producer-grazer ecological model comes into play

$$\begin{cases} \dfrac{dA}{dt} = r(1 - \dfrac{q_0 A}{P_T - q_2 G})A - cA^2 - d_1 A - aAG := \Phi(A, G), \\ \dfrac{dG}{dt} = \hat{e}\min\{1, \dfrac{P_T - q_2 G}{q_2 A}\}aAG - d_2 G := \Psi(A, G). \end{cases} \tag{1}$$

The per capita fertility rate of producer, i.e., $r(1-q_0A/(P_T-q_2G))$, indicates both the intraspecific competition among producers and the interspecific competition for phosphorus between producer and grazer. One must have $r > d_1$. Otherwise, the producer will be extinct and the system collapses.

Define

$$D = \{(A,G)|0 < A < \frac{P_T}{q_0}, G > 0, q_0A + q_2G < P_T\}.$$

It is trivial to show that D is the feasible region of (1) and is positive invariant with respect to (1). The straight line $A + G = P_T/q_2$ divides D into two parts D_1 and D_2, where

$$D_1 = \{(A,G)|0 < A < P_T/q_2, A + G < P_T/q_2\},$$
$$D_2 = \{(A,G)|P_T/q_2 < A < P_T/q_0, A + G > P_T/q_2, q_0A + q_2G < P_T\}.$$

Thus

$$\Psi(A,G) = \begin{cases} (\hat{e}aA - d_2)G, & (A,G) \in D_1, \\ [\frac{\hat{e}a}{q_2}(P_T - q_2G) - d_2]G, & (A,G) \in D_2. \end{cases}$$

The nullcline of producer $\Phi(A,G) = 0$ implies that $A = 0$ and

$$A = \frac{(P_T - q_2G)(r - d_1 - aG)}{c(P_T - q_2G) + rq_0} := N(G).$$

Solve $A = N(G)$ in D, one has

$$G = \frac{aP_T + (r - d_1 - cA)q_2 - \sqrt{\Delta}}{2aq_2} := N^{-1}(A),$$

where $\Delta = [(r - d_1 - cA)q_2 - aP_T]^2 + 4q_0q_2arA$. It is not difficult to show that $G = N^{-1}(A)$ is decreasing with respect to A and passes through $(P_T(r - d_1)/(cP_T + rq_0), 0)$ and $(\min\{P_T/q_2, (r - d_1)/a\}, 0)$. The nullcline of grazer $\Psi(A,G) = 0$ implies that $G = 0$ and $\hat{e}\min\{1, (P_T - q_2G)/(q_2A)\}aA = d_2$, which is equivalent to $A = d_2/(\hat{e}a)$ in D_1 and to $G = P_T/q_2 - d_2/(\hat{e}a)$ in D_2 (see dashed lines in Fig. 1).

Theorem 2.1. *The boundary equilibrium $E_0 = (\bar{A}, 0)$ of (1) always exists and is globally asymptotically stable if one of the following conditions is satisfied*

1. $P_T < d_2q_2/(\hat{e}a)$,
2. $d_2q_2/(\hat{e}a) < rd_2q_0q_2/[(r - d_1)\hat{e}a - cd_2q_2]$ *and* $d_2q_2/(\hat{e}a) < P_T \le rd_2q_0q_2/[(r - d_1)\hat{e}a - cd_2q_2]$.

Proof. (1) always has a boundary equilibrium $E_0 = (\bar{A}, 0)$ with $\bar{A} = (r-d_1)/(rq_0/P_T + c)$. Based on the previous analysis of the nullclines, it is trivial to show that (1) has no positive equilibrium when $P_T < d_2q_2/(\hat{e}a)$ and E_0 is the unique equilibrium of (1). If $0 < \bar{A} \le P_T/q_2$, then the Jacobian of (1) at E_0 reads

$$J(E_0) = \begin{pmatrix} -\frac{rq_0\bar{A}}{P_T} - c\bar{A} & -\frac{rq_0q_2\bar{A}^2}{P_T^2} - a\bar{A} \\ 0 & \hat{e}a\bar{A} - d_2 \end{pmatrix}.$$

If $P_T/q_2 < \bar{A} < P_T/q_0$, then the Jacobian of (1) at E_0 reads

$$J(E_0) = \begin{pmatrix} -\frac{rq_0\bar{A}}{P_T} - c\bar{A} & -\frac{rq_0q_2\bar{A}^2}{P_T^2} - a\bar{A} \\ 0 & \frac{\hat{e}aP_T}{q_2} - d_2 \end{pmatrix}.$$

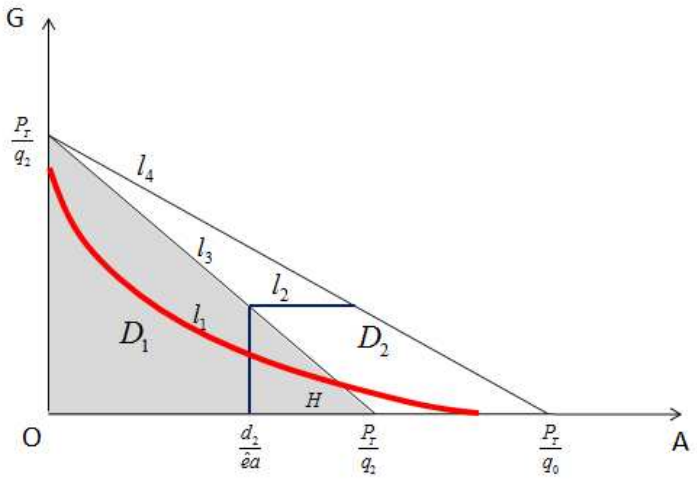

FIGURE 1. The positive invariant set $D = D_1 \cup D_2$ of (1). The red curve l_1 represents $\Phi(A, G)/A = 0$ and the blue lines l_2 denote $\Psi(A, G)/G = 0$. l_3 and l_4 are $q_2A+q_2G = P_T$ and $q_0A+q_2G = P_T$, respectively. $H = (A_H, G_H)$ is the intersection of l_1 and l_3.

Hence, E_0 is locally asymptotically stable when $P_T < d_2q_2/(\hat{e}a)$.

If $P_T > d_2q_2/(\hat{e}a)$ and $\bar{A} \le d_2/\hat{e}a$, then there exists no positive equilibrium of (1) and the Jacobian of (1) at E_0 reads

$$J(E_0) = \begin{pmatrix} -\dfrac{rq_0\bar{A}}{P_T} - c\bar{A} & -\dfrac{rq_0q_2\bar{A}^2}{P_T^2} - a\bar{A} \\ 0 & \hat{e}a\bar{A} - d_2 \end{pmatrix}.$$

Therefore, if $d_2q_2/(\hat{e}a) < P_T \le rd_2q_0q_2/((r-d_1)\hat{e}a - cd_2q_2)$, then E_0 is locally asymptotically stable.

Note that both the A-axes and G-axes are trajectories of (1), so the existence of any periodic orbits is precluded. Therefore, the boundary equilibrium E_0 is globally asymptotically stable for $P_T < \dfrac{d_2q_2}{\hat{e}a}$ and $\dfrac{d_2q_2}{\hat{e}a} < P_T \le \dfrac{rd_2q_0q_2}{(r-d_1)\hat{e}a - cd_2q_2}$ with $\dfrac{d_2q_2}{\hat{e}a} < \dfrac{rd_2q_0q_2}{(r-d_1)\hat{e}a - cd_2q_2}$. □

Based on the above analysis, there exists positive equilibrium of (1) if $P_T > \max\{d_2q_2/(\hat{e}a), rd_2q_0q_2/[(r-d_1)\hat{e}a - cd_2q_2]\}$. For the convenience of discussion, we assume that $d_2q_2/(\hat{e}a) \ge rd_2q_0q_2/[(r-d_1)\hat{e}a - cd_2q_2]$ always holds. Denote the intersection of $\Phi(A, G)/A = 0$ and $A + G = P_T/q_2$ in the first quadrant by $H = (A_H, G_H)$, where

$$A_H = \frac{aP_T + rq_0 - rq_2 + d_1q_2}{(a-c)q_2}.$$

Next, we deal with the existence and stability of the positive equilibrium of (1).

Theorem 2.2. *Assume that $P_T > d_2q_2/(\hat{e}a)$. Then (1) has a unique positive equilibrium $E_1 = (A_1, G_1)$ being globally asymptotically stable. In particular, E_1 lies in D_1 when $A_H > d_2/(\hat{e}a)$ and lies in D_2 when $A_H < d_2/(\hat{e}a)$.*

Proof. The proof of the existence and uniqueness of $E_1 = (A_1, G_1)$ is straightforward. Note that $\Phi(A, G)/A = 0$ is decreasing with respect to A. Then, if $A_H > d_2/(\hat{e}a)$, then E_1 is located in D_1 with $A_1 = d_2/(\hat{e}a)$, and, if $A_H < d_2/(\hat{e}a)$, then E_1 is located in D_2 with $G_1 = P_T/q_2 - d_2/(\hat{e}a)$. If $A_H = d_2/(\hat{e}a)$, then $E_1 = (A_1, G_1) = (d_2/(\hat{e}a), P_T/q_2 - d_2/(\hat{e}a))$.

For the stability of E_1, consider the Jacobian $J(E_1)$ of (1) at E_1. If $A_H < d_2/(\hat{e}a)$, then $J(E_1)$ writes

$$J(E_1) = \begin{pmatrix} -\dfrac{rq_0A_1}{P_T - q_2G_1} - cA_1 & -\dfrac{rq_0q_2A_1^2}{P_T^2} - aA_1 \\ 0 & -\hat{e}aG_1 \end{pmatrix}.$$

If $A_H > d_2/(\hat{e}a)$, then $J(E_1)$ reads

$$J(E_1) = \begin{pmatrix} -\dfrac{rq_0A_1}{P_T - q_2G_1} - cA_1 & -\dfrac{rq_0q_2A_1^2}{P_T^2} - aA_1 \\ \hat{e}aG_1 & 0 \end{pmatrix}.$$

It is not difficult to show that both of the eigenvalues of $J(E_1)$ always have negative real parts. Hence, E_1 is locally asymptotically stable. Furthermore, it is obvious that E_0 is always unstable by the Jacobian of (1) at E_0 when $P_T > d_2q_2/(\hat{e}a)$.

Consider the Dulac function defined by $B(A, G) = 1/(AG)$, then

$$\frac{\partial(B\Phi(A,G))}{\partial A} + \frac{\partial(B\Psi(A,G))}{\partial G} = \begin{cases} -\dfrac{c}{G} - \dfrac{rq_0}{(P_T - q_2G)G}, & (A,G) \in D_1, \\ -\dfrac{c}{G} - \dfrac{rq_0}{(P_T - q_2G)G} - \dfrac{\hat{e}a}{A}, & (A,G) \in D_2. \end{cases}$$

Define

$$\lambda_1 = \min_{(A,G)\in D_1}\{\frac{c}{G} + \frac{rq_0}{(P_T - q_2G)G}\},$$
$$\lambda_2 = \min_{(A,G)\in D_2}\{\frac{c}{G} + \frac{rq_0}{(P_T - q_2G)G} + \frac{\hat{e}a}{A}\}$$

and let $\lambda = \min\{\lambda_1, \lambda_2\}$. Then, λ is obviously positive. Hence, the generalized Dulac's criterion is applied and (1) has no nontrivial periodic solutions in D. Therefore, by the Poincaré-Bendixson theory, $E_1 = (A_1, G_1)$ is globally asymptotically stable when $P_T > d_2q_2/(\hat{e}a)$. □

When $P_T < d_2q_2/(\hat{e}a)$, E_0 is globally asymptotically stable, that is, the grazer is extinct and the producer persists. When $P_T > d_2q_2/(\hat{e}a)$, E_1 is globally asymptotically stable, which implies that both the producer and the grazer coexist. Note that $A_H > d_2/(\hat{e}a)$ is equivalent to

$$P_T > \frac{d_2q_2}{\hat{e}a}(1 - \frac{c}{a}) + \frac{r(q_2 - q_0)}{a} - \frac{d_1q_2}{a}.$$

Therefore, the location of E_1 is also determined by the total phosphorus P_T. In summary, the total phosphorus P_T characterizes the global dynamics of (1), and the producer and grazer coexist for higher phosphorus.

2.2. **The evolutionary model.** Body size is an important factor in a food web, especially for phytoplankton, because it affects the carbon cycling and nutrients availability [16, 29]. In the following, the body size is considered as the evolutionary trait due to its considerable impacts on the metabolism and interactions of organisms[22, 29, 42, 48]. Our study focuses on how the total phosphorus density affects the evolution of body size. Let x_1 and x_2 be the traits of producer and grazer respectively. Although the parameters in (1) are constant in the ecological process, some of them vary with the body sizes in the evolutionary process.

Recent studies show that the per capita maximum growth rate of producer changes with its body size and is a function of body size [22, 37, 38]. For example, for some phytoplankton with relatively large body or cell sizes, the per capita maximum growth rate tends to decline with a decelerating rate as body size increases, whereas for the species with relatively small body size, the per capita maximum growth rate tends to increase with body or cell size [22]. Therefore, we assume that the per capita maximum growth rate r of producer is a Gaussian function of $(x_1 - x_0)$ given by

$$r := r(x_1) = r_0 \exp\{\frac{-(x_1 - x_0)^2}{2\sigma_r^2}\}, \tag{2}$$

where x_0 is the intermediate body size at which the best advantage occurs and r_0 is the producer's maximum growth rate with $x_1 = x_0$ and σ_r^2 is the variance of the phenotypic effect of individuals with trait x_1.

When a mutant producer with trait y_1 is present, suppose that producers with different sizes may take up different nutrients and the competition between them is weaker than that between the ones with the same size [25, 13, 48], so the strength of intraspecific competition of producer (say c) depends on the traits difference and is modeled by

$$c := c(y_1, x_1) = c_0 \exp\{\frac{-(y_1 - x_1)^2}{2\sigma_c^2}\}, \tag{3}$$

where c_0 is the maximum strength of intraspecific competition of producer and σ_c^2 is the variance of the phenotypic effect of individuals with traits y_1 and x_1 interactions.

Usually, the grazer is inefficient to catch and feed on producers with too large or too small body size, and it selectively feeds on the producers that are of certain size to maximize energy gains[22, 29, 48]. So, we assume that the capture rate of grazer is a Gaussian function with a maximum value and is given by

$$a := a(x_1, x_2) = a_0 \exp\{\frac{-(x_1 - \theta x_2)^2}{2\sigma_a^2}\}, \tag{4}$$

where a_0 is the maximum capture rate, θ is a constant that defines grazer selectivity and σ_a^2 is the variance of phenotypic effect of individuals with traits x_1 and x_2 interactions. The capture rate a is maximized at $x_1 = \theta x_2$. In this paper, we assume that $\theta = 1$ always holds for simplification. Therefore, the ecological dynamics of resident producer and grazer populations with traits x_1 and x_2 reads

$$\begin{cases} \dfrac{dA(x_1,t)}{dt} = & A(x_1,t)[r(x_1)(1 - \dfrac{q_0 A(x_1,t)}{P_T - q_2 G(x_2,t)}) - c(x_1,x_1)A(x_1,t) - d_1 \\ & -a(x_1,x_2)G(x_2,t)], \\ \dfrac{dG(x_2,t)}{dt} = & G(x_2,t)[\hat{e}\min\{1, \dfrac{P_T - q_2 G(x_2,t)}{q_2 A(x_1,t)}\}a(x_1,x_2)A(x_1,t) - d_2], \end{cases} \tag{5}$$

where $A(x_1,t)$ is the density of resident producer population with trait value x_1 at time t, $G(x_2,t)$ is the density of resident grazer population with trait value x_2 at time t, and, $r(x_1)$, $c(x_1,x_1)$ and $a(x_1,x_2)$ are defined in (2)-(4).

Define the traits set of (5) for coevolution by

$$X=\{(x_1,x_2)|P_T>\frac{d_2q_2}{\hat{e}a(x_1,x_2)},x_1>0,x_2>0\}.$$

By carrying out similar arguments to those in Theorem 2.2, one concludes that, if $(x_1,x_2)\in X$, then the positive ecological equilibrium $(A^*(x_1,x_2),G^*(x_1,x_2))$ of (5) exists and is globally asymptotically stable, that is, the producer and the grazer can coexist and co-evolve (see Fig. 2). We will deliberately study the coevolution of (5) in X. It is obvious that, when $x_1=x_2=x_0$, $r=r_0$, $c=c_0$, and $a=a_0$, one has $A^*=A_1$ and $G^*=G_1$.

For the convenience of discussion, define

$$A(x_1,x_2):=N(G(x_1,x_2))=\frac{(P_T-q_2G(x_1,x_2))(r(x_1)-d_1-a(x_1,x_2)G(x_1,x_2))}{c(x_1,x_1)(P_T-q_2G(x_1,x_2))+r(x_1)q_0},$$

$$G(x_1,x_2):=N^{-1}(A(x_1,x_2))=\frac{a(x_1,x_2)P_T+(r(x_1)-d_1-c(x_1,x_1)A)q_2-\sqrt{\Delta}}{2a(x_1,x_2)q_2},$$

$$X_1:=\{(x_1,x_2)|\frac{a(x_1,x_2)P_T+r(x_1)(q_0-q_2)+d_1q_2}{(a(x_1,x_2)-c(x_1,x_1))q_2}>\frac{d_2}{\hat{e}a(x_1,x_2)},x_1>0,x_2>0\},$$

$$X_2:=\{(x_1,x_2)|\frac{a(x_1,x_2)P_T+r(x_1)(q_0-q_2)+d_1q_2}{(a(x_1,x_2)-c(x_1,x_1))q_2}<\frac{d_2}{\hat{e}a(x_1,x_2)},x_1>0,x_2>0\},$$

where

$$\Delta=[(r(x_1)-d_1-c(x_1,x_1)A(x_1,x_2))q_2-a(x_1,x_2)P_T]^2$$
$$+4q_0q_2a(x_1,x_2)r(x_1)A(x_1,x_2).$$

When $(x_1,x_2)\in X$, (5) has a unique positive equilibrium (A^*,G^*) with

$$\begin{cases}A^*:=A^*(x_1,x_2)=\begin{cases}\dfrac{d_2}{ea(x_1,x_2)}, & (x_1,x_2)\in X_1,\\ N(G^*), & (x_1,x_2)\in X_2,\end{cases}\\ G^*:=G^*(x_1,x_2)=\begin{cases}N^{-1}(A^*), & (x_1,x_2)\in X_1,\\ \dfrac{P_T}{q_2}-\dfrac{d_2}{\hat{e}a(x_1,x_2)}, & (x_1,x_2)\in X_2.\end{cases}\end{cases}\tag{6}$$

Suppose the mutations in producer and grazer are rare and there is either a mutant producer or a mutant grazer but not both at a time [21, 48]. A significant assumption in the adaptive dynamics is that the time-scale of evolutionary process is much greater than the time scale of ecological process [21, 30]. Consequently, the ecological dynamics first lead (5) to its equilibrium, next the mutations arise, then the two populations reach the steady state before next mutations come out.

Evolutionary process is described by invasion fitness. The fitness of a mutant is defined by its long-term per capita growth rate in the resident population and the mutant can spread if its fitness is positive [9, 21]. The fitness of a mutant producer with trait y_1 in the resident populations is given by

$$f_1(y_1,x_1,x_2)=\frac{dA(y_1,t)}{Adt}=r(y_1)(1-\frac{q_0A^*}{P_T-q_2G^*})-d_1-c(y_1,x_1)A^*-a(y_1,x_2)G^*.$$

The mutant producer can grow in the resident producer population if $f_1(y_1,x_1,x_2)>0$. Similarly, the fitness of a mutant grazer with trait y_2 in the resident populations

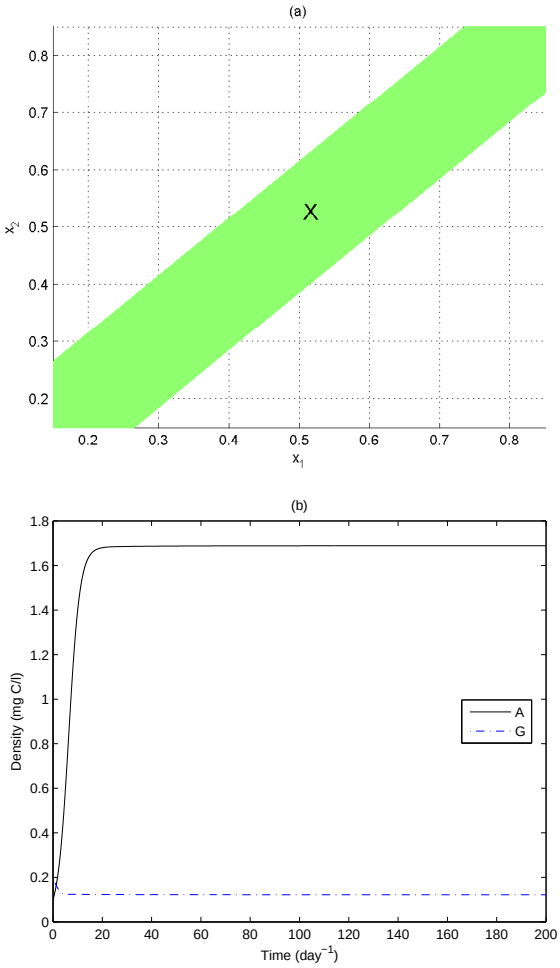

FIGURE 2. (a) X is the traits set for coevolution of (5). If $(x_1, x_2) \in X$, then (5) has a globally asymptotically stable positive equilibrium (A^*, G^*), which implies that the producer and grazer coexist and co-evolve. (b)The positive equilibrium (A^*, G^*) is globally asymptotically stable with the traits $x_1 = 0.4$ and $x_2 = 0.3$. The parameter values are listed in Table 1.

can be described by

$$f_2(y_2, x_1, x_2) = \frac{dG(y_2, t)}{Gdt} = ea(x_1, y_2)A^* - d_2,$$

where $e = \hat{e}\min\{1, (P_T - q_2G^*)/(q_2A^*)\}$.

The fitness gradient is the derivative of the fitness with respect to mutant trait value at the resident trait value and determines the direction in which the trait

evolves [21, 30]. Therefore, the fitness gradients $g_1(x_1, x_2)$ and $g_2(x_1, x_2)$ reads

$$\begin{aligned} g_1(x_1,x_2) = & \frac{\partial f_1(y_1,x_1,x_2)}{\partial y_1}|_{y_1=x_1} = -\frac{(x_1-x_0)r(x_1)}{\sigma_r^2}(1-\frac{q_0A^*}{P_T-q_2G^*}) \\ & +\frac{(x_1-x_2)a(x_1,x_2)G^*}{\sigma_a^2}, \\ g_2(x_1,x_2) = & \frac{\partial f_2(y_2,x_1,x_2)}{\partial y_2}|_{y_2=x_2} = \frac{(x_1-x_2)ea(x_1,x_2)A^*}{\sigma_a^2}. \end{aligned} \tag{7}$$

If $g_i(x_1, x_2) > 0 (i = 1, 2)$, then invasion fitness increases for mutants with trait value $y_i (i = 1, 2)$. Since $f_i(x_i, x_1, x_2) = 0 (i = 1, 2)$, by necessity (i.e., the resident neither grows nor declines in its own equilibrium population), mutants with higher trait values can invade and are favored by natural selection, while mutants with lower trait values are selected against [13].

According to [9], if the mutations are random and rare, the evolutionary model of traits x_1 and x_2 can be written into

$$\begin{cases} \dfrac{dx_1}{dt} = m_1(x_1,x_2)g_1(x_1,x_2), \\ \dfrac{dx_2}{dt} = m_2(x_1,x_2)g_2(x_1,x_2), \end{cases} \tag{8}$$

where $m_1(x_1, x_2) = \mu_1{\sigma_1}^2 A^*/2$, $m_2(x_1, x_2) = \mu_2{\sigma_2}^2 G^*/2$, $\mu_i (i = 1, 2)$ are the probabilities that the birth events are mutant for producer and grazer respectively, $\sigma_i^2 (i = 1, 2)$ are the variances of the mutation distribution of producer and grazer respectively and are assumed to be constants.

3. Evolutionary outcomes without grazer.

We first introduce some basic concepts in adaptive dynamics. One can find more details in [21]. Evolutionary singular point is a trait value at which the locally fitness gradient is zero. The singular points are classified by evolutionary stable strategy (ESS), convergence stability, continuously stable strategy (CSS) and evolutionary branching point. ESS-stability means a singular point can not be invaded by nearby mutants. A singular point is convergence stable if a population of a nearby phenotype can be invaded by mutants that are even closer to the singular point. If the singular point is both convergence stable and ESS-stable, we call it CSS-stable. If the singular point is convergence stable but not ESS-stable, and the initially monomorphic population becomes dimorphism on the long run, we call it an evolutionary branching point.

In this section, we explore CSS-stability and evolutionary branching for the producer with grazer absent. Our results suggest that the producer population evolves to continuously stable strategy if the total phosphorus density is relatively low, while if the total phosphorus density is relatively high, the producer population evolves to an evolutionary branching point.

In the absence of grazer, the ecological model of the resident producer with trait x_1 becomes

$$\frac{dA(x_1,t)}{dt} = A(x_1,t)[r(x_1)(1-\frac{q_0A(x_1,t)}{P_T}) - c(x_1,x_1)A(x_1,t) - d_1]. \tag{9}$$

Since $r > d_1$, there exists an asymptotically stable equilibrium $\widetilde{A}$ of (9), where

$$\widetilde{A} := \widetilde{A}(x_1) = \frac{(r(x_1)-d_1)P_T}{c(x_1,x_1)P_T + r(x_1)q_0}.$$

It is observed that $\widetilde{A} = \bar{A}$ when $x_1 = x_0$, $r = r_0$ and $c = c_0$. When the grazer is absent, the fitness for the mutant producer is

$$f_{11}(y_1, x_1) = r(y_1)(1 - \frac{q_0\widetilde{A}}{P_T}) - c(y_1, x_1)\widetilde{A} - d_1.$$

The fitness gradient is

$$g_{11}(x_1) = \frac{\partial f_{11}(y_1, x_1)}{\partial y_1}|_{y_1=x_1} = -\frac{(x_1 - x_0)r(x_1)}{{\sigma_r}^2}(1 - \frac{q_0\widetilde{A}}{P_T}).$$

So the evolutionary model of the trait x_1 is

$$\frac{dx_1}{dt} = \frac{1}{2}\mu_1{\sigma_1}^2\widetilde{A}g_{11}(x_1). \tag{10}$$

By (10), it is not difficult to show that ${x_1}^* = x_0$ is the evolutionarily singular point and is always convergence stable since

$$\frac{dg_{11}(x_1)}{dx_1} = -\frac{r(x_1)}{\sigma_r^2}(1 - \frac{q_0\widetilde{A}}{P_T}) + \frac{(x_1 - x_0)^2 r(x_1)}{{\sigma_r}^4}(1 - \frac{q_0\widetilde{A}}{P_T})$$

and

$$\frac{dg_{11}(x_1)}{dx_1}|_{x_1=x_0} < 0.$$

When the grazer is absent, the producer evolves to the strategy $x_1^* = x_0$, which means that the producer achieves the maximum growth rate.

Next we consider the second derivative of the mutant fitness with respect to mutant trait value to demonstrate the ESS-stability. Direct calculations lead to

$$\frac{\partial f_{11}^2(y_1, x_1)}{\partial y_1^2}|_{y_1=x_1=x_0} = -\frac{r_0}{{\sigma_r}^2}(1 - \frac{q_0\bar{A}}{P_T}) + \frac{c_0}{{\sigma_c}^2}\bar{A}.$$

If $[\partial f_{11}^2(y_1, x_1)/\partial y_1^2]|_{y_1=x_1=x_0} < 0$, then x_0 is ESS-stable. It follows that the evolutionary attractor x_0 is CSS-stable if

$$(r_0 - d_1)\frac{c_0{\sigma_r}^2}{{\sigma_c}^2} - r_0c_0 < \frac{d_1r_0q_0}{P_T}.$$

If $[\partial f_{11}^2(y_1, x_1)/\partial y_1^2]|_{y_1=x_1=x_0} > 0$, then x_0 is not ESS-stable and it is an evolutionary branching point when

$$\frac{\partial f_{11}^2(y_1, x_1)}{\partial y_1^2}|_{y_1=x_1=x_0} + \frac{\partial f_{11}^2(y_1, x_1)}{\partial x_1^2}|_{y_1=x_1=x_0} > 0.$$

Note that

$$\frac{\partial f_{11}^2(y_1, x_1)}{\partial x_1^2}|_{y_1=x_1=x_0} = \frac{c_0}{{\sigma_c}^2}\bar{A},$$

we reach the following claim on the continuously stable strategy and the evolutionary branching of (9).

Theorem 3.1. *Assume that $r_0 > d_1$.*

1. *The evolutionarily singular point x_0 is CSS-stable if $(r_0 - d_1){\sigma_r}^2 \le r_0{\sigma_c}^2$.*
2. *The evolutionarily singular point x_0 is CSS-stable if $(r_0 - d_1){\sigma_r}^2 > r_0{\sigma_c}^2$ and $P_T < d_1r_0q_0{\sigma_c}^2/[(r_0 - d_1)c_0{\sigma_r}^2 - r_0c_0{\sigma_c}^2]$.*
3. *The evolutionarily singular point x_0 is an evolutionary branching point if $(r_0 - d_1){\sigma_r}^2 > r_0{\sigma_c}^2$ and $P_T > d_1r_0q_0{\sigma_c}^2/[(r_0 - d_1)c_0{\sigma_r}^2 - r_0c_0{\sigma_c}^2]$.*

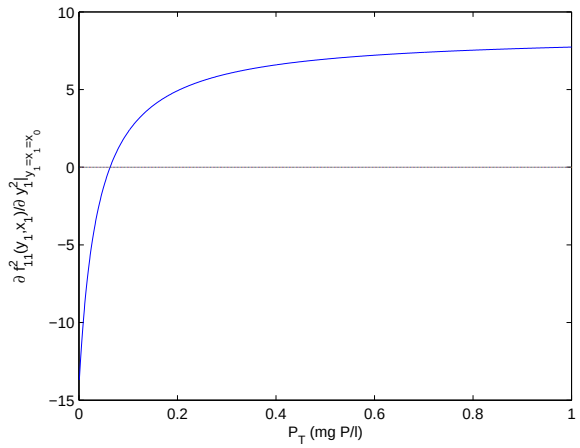

FIGURE 3. The graph of $[\partial f_{11}^2(y_1, x_1)/\partial y_1^2]|_{y_1=x_1=x_0}$ versus P_T. When $[\partial f_{11}^2(y_1, x_1)/\partial y_1^2]|_{y_1=x_1=x_0} < 0$, the singular point x_0 is ESS-stable; when $[\partial f_{11}^2(y_1, x_1)/\partial y_1^2]|_{y_1=x_1=x_0} > 0$, it is an evolutionary branching point. All the parameters values are listed in Table 1.

From Theorem 3.1, it follows that, if $(r_0 - d_1){\sigma_r}^2 \leq r_0{\sigma_c}^2$, then the singular point x_0 is always CSS-stable no matter how much the total phosphorus density P_T is; if $(r_0 - d_1){\sigma_r}^2 > r_0{\sigma_c}^2$, then the producer population will evolve to the CSS-stability with relatively low P_T, and evolve to an evolutionary branching point with relatively high P_T. The graph of $[\partial f_{11}^2(y_1, x_1)/\partial y_1^2]|_{y_1=x_1=x_0}$ versus P_T for $(r_0 - d_1){\sigma_r}^2 > r_0{\sigma_c}^2$ is presented in Fig. 3 and it is increasing with respect to P_T. Pairwise invasibility plot can be used to analyze the evolution of a monomorphic population[21]. For one strategy x of the resident, when the vertical line through x lies in the region where the population's mutant fitness is positive, it implies potentially invading mutants. While the vertical line through x lies in the region where the population's mutant fitness is negative, it means impossibly invading mutants. In Fig. 4, the singular point x_0 is CSS-stable and the producer population evolves to a monomorphic population for $P_T = 0.04$, and the singular point x_0 is an evolutionary branching point and the producer population splits up into two divergence sub-populations for $P_T = 1$.

Our studies suggest that the total phosphorus density exerts a considerable influence on the producer evolution. When the grazer is absent, the increasing of the total phosphorus density leads to the producer population undergoing CSS-stability first and then evolutionary branching.

4. **Co-evolutionary outcomes.** In this section, we devote to investigating the effects of the total phosphorus density on the coevolution dynamics of (8) when grazer is present. In particular, it shows, with the increasing of the total phosphorus, the producer and grazer may co-evolve from CSS-stability to evolutionary branching if the singular point is convergence stable. Moreover, if the mutants whose invasion fitness is larger than zero not only invade but also replace the former resident, then the producer and grazer may evolve into an evolutionary cycle, which is a likely

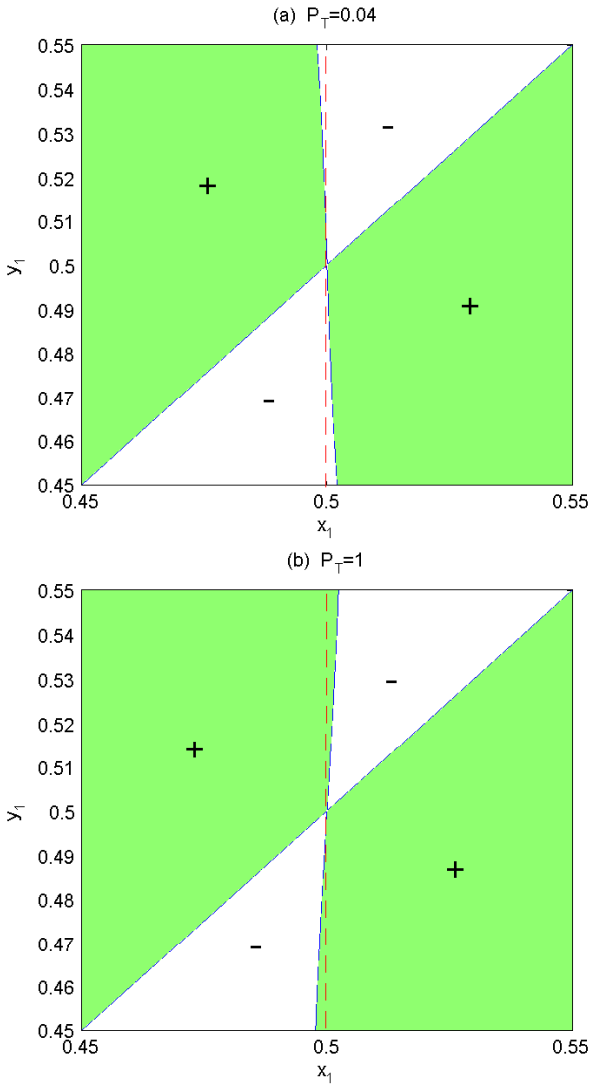

FIGURE 4. Pairwise invasibility plot in the absence of grazers. Mutant traits values of producer are denoted by y_1 and resident traits values of producer by x_1. The producer's mutant fitness $f_{11}(y_1, x_1)$ is positive when (x_1, y_1) is located in the shaded area, which means that the mutant with trait y_1 can invade. The producer's mutant fitness $f_{11}(y_1, x_1)$ is negative when (x_1, y_1) is located in the unshaded area, which means that the mutant with trait y_1 can not invade. (a) For $P_T = 0.04$, the vertical line through x_0 completely locates inside the unshaded region and then x_0 is ESS-stable. (b) For $P_T = 1$, the vertical line through x_0 locates completely inside the shaded region and then x_0 is an evolutionary branching point. The parameter values are listed in Table 1 except P_T.

evolutionary outcome representing that the species coexist with cyclic changes in traits values [10, 48]. The existence and stability of the evolutionary cycle are obtained by bifurcation theory. Numerical simulations reveal that the coevolutionary process is sensitive to the initial condition under high phosphorus density.

4.1. **Continuously stable strategy.** The Jacobian of (8) at (x_1, x_2) reads

$$J(x_1,x_2)=\begin{pmatrix} m_1\dfrac{\partial g_1}{\partial x_1} & m_1\dfrac{\partial g_1}{\partial x_2} \\ m_2\dfrac{\partial g_2}{\partial x_1} & m_2\dfrac{\partial g_2}{\partial x_2} \end{pmatrix},$$

where

$$\begin{aligned}
\frac{\partial g_1}{\partial x_1}&=[-\frac{1}{\sigma_r^2}+\frac{(x_1-x_0)^2}{\sigma_r^4}]r(x_1)(1-\frac{q_0A^*}{P_T-q_2G^*})+[\frac{1}{\sigma_a^2}-\frac{(x_1-x_2)^2}{\sigma_a^4}]a(x_1,x_2)G^*,\\
\frac{\partial g_1}{\partial x_2}&=[-\frac{1}{\sigma_a^2}+\frac{(x_1-x_2)^2}{\sigma_a^4}]a(x_1,x_2)G^*,\\
\frac{\partial g_2}{\partial x_1}&=[\frac{1}{\sigma_a^2}-\frac{(x_1-x_2)^2}{\sigma_a^4}]ea(x_1,x_2)A^*,\\
\frac{\partial g_2}{\partial x_2}&=[-\frac{1}{\sigma_a^2}+\frac{(x_1-x_2)^2}{\sigma_a^4}]ea(x_1,x_2)A^*,
\end{aligned}$$

and $e=\hat{e}\min\{1,(P_T-q_2G^*)/(q_2A^*)\}$. The evolutionary model (8) has a unique singular point (x_1^*,x_2^*) with $x_1^*=x_2^*=x_0$. Let $A_0^*=A^*(x_0,x_0)$, $G_0^*=G^*(x_0,x_0)$, $m_1=\mu_1\sigma_1^2A_0^*/2$, $m_2=\mu_2\sigma_2^2G_0^*/2$. Then

$$J(x_0,x_0)=\begin{pmatrix} m_1[-\dfrac{r_0}{\sigma_r^2}(1-\dfrac{q_0A_0^*}{P_T-q_2G_0^*})+\dfrac{a_0}{\sigma_a^2}G_0^*] & -\dfrac{m_1a_0G_0^*}{\sigma_a^2} \\ \dfrac{m_2ea_0A_0^*}{\sigma_a^2} & -\dfrac{m_2ea_0A_0^*}{\sigma_a^2} \end{pmatrix}$$

and

$$\begin{aligned}
\det(J(x_0,x_0)) &= \frac{m_1m_2ea_0r_0A_0^*}{\sigma_r^2\sigma_a^2}(1-\frac{q_0A_0^*}{P_T-q_2G_0^*})>0,\\
\mathrm{Tr}(J(x_0,x_0)) &= \frac{1}{2}A_0^*[-\frac{\mu_1\sigma_1^2}{\sigma_r^2}(d_1+c_0A_0^*)+(\frac{\mu_1\sigma_1^2}{\sigma_a^2}-\frac{\mu_1\sigma_1^2}{\sigma_r^2}-\frac{e\mu_2\sigma_2^2}{\sigma_a^2})a_0G_0^*],
\end{aligned}$$

where $r_0[1-q_0A_0^*/(P_T-q_2G_0^*)]=d_1+c_0A_0^*+a_0G_0^*$ has been used.

For simplification, denote the two critical values of P_T by P_T^1 and P_T^2, where

$$P_T^1=\frac{d_2q_2}{\hat{e}a_0},\ P_T^2=q_2[\frac{d_2}{\hat{e}a_0}(1-\frac{c_0}{a_0})+\frac{r_0}{a_0}(1-\frac{q_0}{q_2})-\frac{d_1}{a_0}]. \tag{11}$$

We only study the evolutionary model (8) for $P_T^1<P_T^2$ since E_1 is always located in D_1 when $P_T^1\geq P_T^2$ and the results can be deduced in the same way for $P_T^1<P_T^2$.

We first discuss the convergence stability of $(x_0,x_0)\in X_1$, which means that $P_T>P_T^2$ and $e=\hat{e}$. It is obvious that $\mathrm{Tr}(J(x_0,x_0))$ is always negative when $\mu_1\sigma_1^2\sigma_r^2\leq\mu_1\sigma_1^2\sigma_a^2+\hat{e}\mu_2\sigma_2^2\sigma_r^2$. If $\mu_1\sigma_1^2\sigma_r^2>\mu_1\sigma_1^2\sigma_a^2+\hat{e}\mu_2\sigma_2^2\sigma_r^2$, then $\mathrm{Tr}(J(x_0,x_0))$ is negative for $G_0^*<G_{c1}$, where

$$G_{c1}=\frac{\mu_1\sigma_1^2\sigma_a^2(\hat{e}a_0d_1+c_0d_2)}{\hat{e}a_0^2(\mu_1\sigma_1^2\sigma_r^2-\mu_1\sigma_1^2\sigma_a^2-\hat{e}\mu_2\sigma_2^2\sigma_r^2)}.$$

By the properties of $G = N^{-1}(A)$, G_0^* is monotonically increasing with respect to P_T and there exists a unique

$$P_T{}^{c1} = q_2 G_{c1} + \frac{r_0 q_0 d_2}{e a_0 (r_0 - d_1 - a_0 G_{c1}) - c_0 d_2}$$

such that $G_0^* = G_{c1}$. If $P_T^{c1} > P_T^2$, then $\mathrm{Tr}(J(x_0, x_0)) < 0$ for $P_T^2 < P_T < P_T^{c1}$. Now, the convergence stability of $(x_0, x_0) \in X_1$ is summarized in the following theorem.

Theorem 4.1. *Assume that $P_T > P_T^2$. Then the singular point (x_0, x_0) of (8) is convergence stable if one of the following conditions is satisfied*

1. $\mu_1 \sigma_1^2 \sigma_r^2 \le \mu_1 \sigma_1^2 \sigma_a^2 + e\mu_2 \sigma_2^2 \sigma_r^2$,
2. $\mu_1 \sigma_1^2 \sigma_r^2 > \mu_1 \sigma_1^2 \sigma_a^2 + e\mu_2 \sigma_2^2 \sigma_r^2$, $P_T^2 < P_T{}^{c1}$, $P_T^2 < P_T < P_T{}^{c1}$.

Theorem 4.1 characterizes the effect of total phosphorus on the convergence stability of the singular point $(x_0, x_0) \in X_1$. The first claim in Theorem 4.1 shows that the convergence stability of the singular point (x_0, x_0) is independent of P_T. In the second claim, the convergence stability of (x_0, x_0) depends on P_T and is convergence stable for lower P_T. The increasing of P_T is negative to the convergence stability of the singular point (x_0, x_0). Fig. 5 shows an example that the singular point (x_0, x_0) is convergence stable for $0.0335 < P_T < 0.2866$ and is not convergence stable for $P_T > 0.2866$. In fact, $P_T > P_T^2 = 0.0335$ guarantees that the positive ecological equilibrium (N^*, P^*) is asymptotically stable at $(x_0, x_0) \in X_1$.

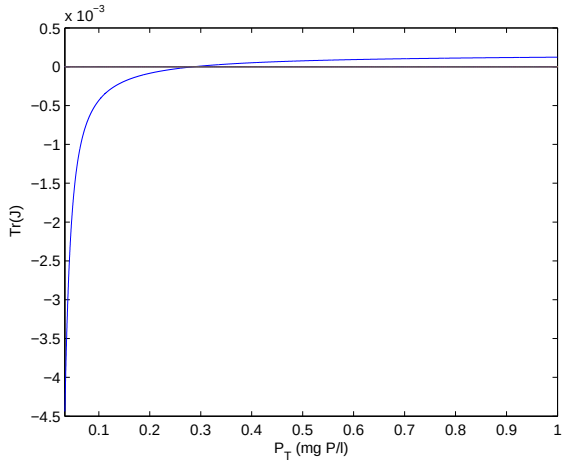

FIGURE 5. The graph of $Tr(J(x_0, x_0))$ versus P_T with $P_T > P_T^2$. The singular point (x_0, x_0) is convergence stable when $Tr(J)$ is negative and is not convergence stable when $Tr(J)$ is positive. Parameters values are listed in Table 1 except $\sigma_r^2 = 0.013$, $\sigma_c^2 = 0.015$, $\sigma_a^2 = 0.0099$, $\sigma_2^2 = 0.001$.

Next, we discuss the convergence stability of $(x_0, x_0) \in X_2$, which means that $P_T^1 < P_T < P_T^2$ and $e = \hat{e}(P_T - q_2 G_0^*)/(q_2 A_0^*)$. It is obvious that, if $\sigma_r^2 \le \sigma_a^2$, then

$\mathrm{Tr}(J(x_0,x_0))<0$. If $\sigma_r^2>\sigma_a^2$, then

$$\begin{aligned}\mathrm{Tr}(J(x_0,x_0)) &= \frac{1}{2}A_0^*[-\frac{\mu_1\sigma_1^2}{\sigma_r^2}(d_1+c_0A_0^*)+(\frac{\mu_1\sigma_1^2}{\sigma_a^2}-\frac{\mu_1\sigma_1^2}{\sigma_r^2})a_0G_0^*-\frac{ea_0\mu_2\sigma_2^2}{\sigma_a^2}G_0^*]\\ &= \frac{1}{2}A_0^*[-\frac{\mu_1\sigma_1^2}{\sigma_r^2}(d_1+c_0A_0^*)+(\frac{\mu_1\sigma_1^2}{\sigma_a^2}-\frac{\mu_1\sigma_1^2}{\sigma_r^2})a_0G_0^*-\frac{\mu_2\sigma_2^2d_2}{\sigma_a^2}\frac{G_0^*}{A_0^*}]\end{aligned}$$

for $G_0^*=P_T/q_2-d_2/\hat{e}a$. Note that

$$A_0^*=\frac{d_2q_2(r_0-d_1-a_0G_0^*)}{c_0d_2q_2+r_0\hat{e}a_0q_0}:=\alpha-\beta G_0^*, \tag{12}$$

where $\alpha=d_2q_2(r_0-d_1)/(c_0d_2q_2+r_0\hat{e}a_0q_0)$, $\beta=d_2q_2a_0/(c_0d_2q_2+r_0\hat{e}a_0q_0)$, and $G_0^*<\alpha/\beta$. Then

$$\begin{aligned}\mathrm{sgn}(\mathrm{Tr}(J(x_0,x_0))) &= \mathrm{sgn}((\alpha-\beta G_0^*)\{-\frac{\mu_1\sigma_1^2}{\sigma_r^2}[d_1+c_0(\alpha-\beta G_0^*)]\\ &\quad +(\frac{\mu_1\sigma_1^2}{\sigma_a^2}-\frac{\mu_1\sigma_1^2}{\sigma_r^2})a_0G_0^*\}-\frac{\mu_2\sigma_2^2d_2}{\sigma_a^2}G_0^*)\\ &= \mathrm{sgn}((\alpha-\beta G_0^*)(G_0^*-\gamma)-\delta G_0^*)\\ &= \mathrm{sgn}(-\beta {G_0^*}^2+(\alpha+\beta\gamma-\delta)G_0^*-\alpha\gamma),\end{aligned}$$

where

$$\gamma=\frac{\sigma_a^2(d_1+c_0\alpha)}{\sigma_a^2c_0\beta+(\sigma_r^2-\sigma_a^2)a_0}>0,\ \delta=\frac{\mu_2\sigma_2^2d_2\sigma_r^2}{\mu_1\sigma_1^2(\sigma_a^2c_0\beta+(\sigma_r^2-\sigma_a^2)a_0)}>0.$$

If $1<\sigma_r^2/\sigma_a^2\le r_0/(r_0-d_1)$, then $\gamma\ge\alpha/\beta$ and $\mathrm{Tr}(J(x_0,x_0))<0$ since $G_0^*<\alpha/\beta<\gamma$. If $\sigma_r^2/\sigma_a^2>r_0/(r_0-d_1)$ and $(\alpha+\beta\gamma-\delta)^2-4\alpha\beta\gamma<0$, then $\gamma<\alpha/\beta$ and $\mathrm{Tr}(J(x_0,x_0))<0$. If $\sigma_r^2/\sigma_a^2>r_0/(r_0-d_1)$ and $(\alpha+\beta\gamma-\delta)^2-4\alpha\beta\gamma>0$, then the equation

$$-\beta {G_0^*}^2+(\alpha+\beta\gamma-\delta)G_0^*-\alpha\gamma=0$$

has two positive roots G_{c2} and G_{c3} with $G_{c2}<G_{c3}$. Whence, $\mathrm{Tr}(J(x_0,x_0))<0$ for $G_0^*<G_{c2}$ and $G_0^*>G_{c3}$, $\mathrm{Tr}(J(x_0,x_0))>0$ for $G_{c2}<G_0^*<G_{c3}$. Since G_0^* is increasing with respect to P_T, there exist P_T^{c2} and P_T^{c3} such that $G_0^*=G_{c2}$ and $G_0^*=G_{c3}$. For $P_T<P_T^1$, one has $G_0^*=0$ and $\mathrm{Tr}(J(x_0,x_0))<0$, hence $P_T^1<P_T^{c2}$. If $P_T^2\le P_T^{c2}$, then $\mathrm{Tr}(J(x_0,x_0))<0$ for $P_T^1<P_T<P_T^2$. If $P_T^{c2}<P_T^2\le P_T^{c3}$, then $\mathrm{Tr}(J(x_0,x_0))<0$ for $P_T^1<P_T<P_T^{c2}$ and $\mathrm{Tr}(J(x_0,x_0))>0$ for $P_T^{c2}<P_T<P_T^2$. If $P_T^2>P_T^{c3}$, then $\mathrm{Tr}(J(x_0,x_0))<0$ for $P_T^1<P_T<P_T^{c2}$ and $P_T^{c3}<P_T<P_T^2$, and $\mathrm{Tr}(J(x_0,x_0))>0$ for $P_T^{c2}<P_T<P_T^{c3}$.

Summarize up the above discussion, we reach the following theorem on the convergence stability of the singular point $(x_0,x_0)\in X_2$ of (8).

Theorem 4.2. *Assume that $P_T^1<P_T<P_T^2$. Then the singular point (x_0,x_0) of (8) is convergence stable if one of the following conditions is satisfied*

1. $\sigma_r^2\le\sigma_a^2$;
2. $1<\dfrac{\sigma_r^2}{\sigma_a^2}\le\dfrac{r_0}{r_0-d_1}$;
3. $\dfrac{\sigma_r^2}{\sigma_a^2}>\dfrac{r_0}{r_0-d_1}$,$(\alpha+\beta\gamma-\delta)^2-4\alpha\beta\gamma<0$;
4. $\dfrac{\sigma_r^2}{\sigma_a^2}>\dfrac{r_0}{r_0-d_1}$, $(\alpha+\beta\gamma-\delta)^2-4\alpha\beta\gamma>0$, $P_T^2\le P_T^{c2}$;
5. $\dfrac{\sigma_r^2}{\sigma_a^2}>\dfrac{r_0}{r_0-d_1}$, $(\alpha+\beta\gamma-\delta)^2-4\alpha\beta\gamma>0$, $P_T^{c2}<P_T^2\le P_T^{c3}$, $P_T^1<P_T<P_T^{c2}$;

6. $\frac{\sigma_r^2}{\sigma_a^2} > \frac{r_0}{r_0 - d_1}$, $(\alpha + \beta\gamma - \delta)^2 - 4\alpha\beta\gamma > 0$, $P_T^2 > P_T^{c3}$, $P_T^1 < P_T < P_T^{c2}$ *and* $P_T^{c3} < P_T < P_T^2$.

Theorem 4.2 characterizes the effect of total phosphorus on the convergence stability of the singular point $(x_0, x_0) \in X_2$. The first four claims in Theorem 4.2 show that the convergence stability of the singular point (x_0, x_0) is independent of P_T. In the fifth claim, the convergence stability of (x_0, x_0) depends on P_T, (x_0, x_0) is convergence stable for lower P_T and the increasing of P_T is negative to the convergence stability of the singular point (x_0, x_0). Fig. 6 (a) shows an example that, the singular point (x_0, x_0) is convergence stable for $0.0094 < P_T < 0.0292$ and is not convergence stable for $0.0292 < P_T < 0.0335$, here $P_T^1 = 0.0094$, $P_T^{c2} = 0.0292$ and $P_T^2 = 0.0335$. The sixth claim implies that the increasing of phosphorus may possibly destabilize or stabilize the evolutionary system. Fig.6 (b) shows that (x_0, x_0) is convergence stable for $P_T^1 < P_T < P_T^{c2}$ and $P_T^{c3} < P_T < P_T^2$, where $P_T^1 = 0.000469$, $P_T^{c2} = 0.0191$, $P_T^{c3} = 0.0237$, and $P_T^2 = 0.0253$.

Next we go ahead with the ESS-stability and CSS-stability of (x_0, x_0).

Theorem 4.3. *Assume that* $P_T > P_T^2$. *Let*

$$G_{e1} = \frac{\sigma_a^2[c_0 d_2(\sigma_r^2 - \sigma_c^2) - e a_0 d_1 \sigma_c^2]}{e a_0^2 \sigma_c^2(\sigma_a^2 - \sigma_r^2)}, \quad {P_T}^{e1} = q_2 G_{e1} + \frac{r_0 q_0 d_2}{e a_0(r_0 - d_1 - a_0 G_{e1}) - c_0 d_2}.$$

Then the singular point (x_0, x_0) *is ESS-stable if the one of the following conditions holds*

1. $\sigma_a = \sigma_r$ *and* $c_0 d_2(\sigma_r^2 - \sigma_c^2) < e a_0 d_1 \sigma_c^2$,
2. $\sigma_a > \sigma_r$ *and* $c_0 d_2(\sigma_r^2 - \sigma_c^2) \le e a_0 d_1 \sigma_c^2$,
3. $\sigma_a < \sigma_r$, $c_0 d_2(\sigma_r^2 - \sigma_c^2) < e a_0 d_1 \sigma_c^2$, $P_T^2 < {P_T}^{e1}$, $P_T^2 < P_T < {P_T}^{e1}$,
4. $\sigma_a > \sigma_r$, $c_0 d_2(\sigma_r^2 - \sigma_c^2) > e a_0 d_1 \sigma_c^2$, $P_T > \max\{{P_T}^{e1}, P_T^2\}$.

Proof. Direct calculations produce

$$\begin{aligned}
\frac{\partial^2 f_1(y_1, x_1, x_2)}{\partial y_1^2} &= [-\frac{1}{\sigma_r^2} + \frac{(y_1 - x_0)^2}{\sigma_r^4}] r(y_1)(1 - \frac{q_0 A^*}{P_T - q_2 G^*}) \\
&\quad + [\frac{1}{\sigma_c^2} - \frac{(y_1 - x_1)^2}{\sigma_c^4}] c(x_1, y_1) A^* + [\frac{1}{\sigma_a^2} - \frac{(y_1 - x_2)^2}{\sigma_a^4}] a(y_1, x_2) G^*, \\
\frac{\partial^2 f_2(y_2, x_1, x_2)}{\partial y_2^2} &= [-\frac{1}{\sigma_a^2} + \frac{(y_2 - x_1)^2}{\sigma_a^4}] e a(x_1, y_2) A^*,
\end{aligned}$$

Since $P_T > P_T^2$, one has $A_0^* = d_2/(\hat{e} a_0)$, then

$$\begin{aligned}
\frac{\partial^2 f_1(y_1, x_1, x_2)}{\partial y_1^2} \Big|_{y_1 = x_1 = x_2 = x_0} &= (\frac{a_0}{\sigma_a^2} - \frac{a_0}{\sigma_r^2}) G_0^* + (\frac{c_0}{\sigma_c^2} - \frac{c_0}{\sigma_r^2}) \frac{d_2}{e a_0} - \frac{d_1}{\sigma_r^2}, \\
\frac{\partial^2 f_2(y_2, x_1, x_2)}{\partial y_2^2} \Big|_{y_2 = x_1 = x_2 = x_0} &= -\frac{e a_0}{\sigma_a^2} A_0^* < 0.
\end{aligned}$$

For convenience, denote $I_e := [\partial^2 f_1(y_1, x_1, x_2)/\partial y_1^2]|_{y_1 = x_1 = x_2 = x_0}$. When the first two claims hold, it is obvious that I_e is always negative and the singular point (x_0, x_0) is always ESS-stable. When the third claim holds, by carrying out similar arguments as those in Theorem 4.1, there exists a unique ${P_T}^{e1}$ such that $G_0^* = G_{e1}$. Then $G_0^* < G_{e1}$ for $P_T^2 < P_T < {P_T}^{e1}$, so $I_e < 0$ and the singular point (x_0, x_0) is ESS-stable. If the fourth claim holds, when $P_T > {P_T}^{e1}$, one has $I_e < 0$. Therefore, the singular point (x_0, x_0) is ESS-stable for $P_T > \max\{{P_T}^{e1}, P_T^2\}$. The proof is complete. □

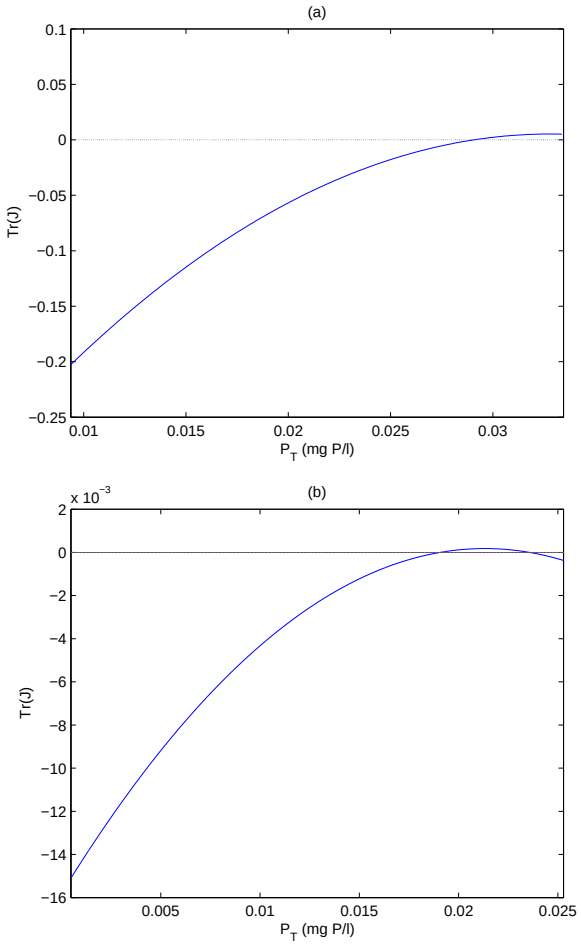

FIGURE 6. The graph of $Tr(J(x_0, x_0))$ versus P_T with $P_T^1 < P_T < P_T^2$. The singular point (x_0, x_0) is convergence stable when $Tr(J)$ is negative and is not convergence stable when $Tr(J)$ is positive. (a) The fifth claim in Theorem 4.2 holds and the parameter values are listed in Table 1. (b) The sixth claim in Theorem 4.2 holds and the parameter values are listed in Table 1 except $d_1 = 0.21$, $d_2 = 0.01$ and $\sigma_2^2 = 0.023$

Theorem 4.3 shows that the singular point $(x_0, x_0) \in X_1$ is always ESS-stable if one of the first two conditions holds. If the third condition is valid, then the singular point (x_0, x_0) is ESS-stable with lower P_T and is not ESS-stable with higher P_T(Fig. 7(a)) . The singular point (x_0, x_0) is ESS-stable with higher P_T and is not ESS-stable with lower P_T when the fourth condition holds(Fig. 7(b)). From Theorem 4.1 and 4.3, it is not difficult to establish sufficient criteria for the CSS-stability of (x_0, x_0). It follows that the total phosphorus affects the convergence stability, ESS-stability of (x_0, x_0), and hence its CSS-stability. Fig. 5 and Fig. 7(a) reveals that the singular point (x_0, x_0) is CSS-stable for $0.0335 < P_T < 0.0347$.

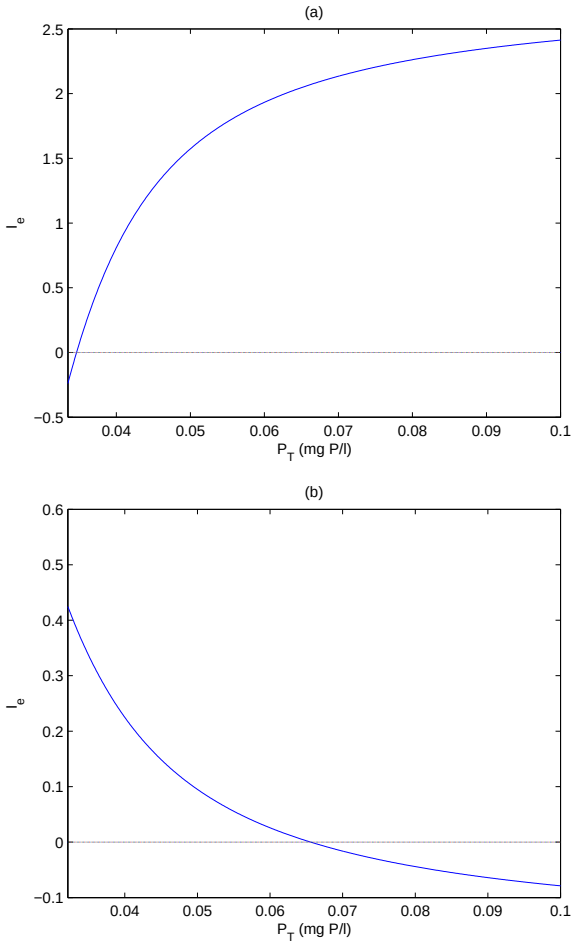

FIGURE 7. The graph of I_e versus P_T with $P_T > P_T^2$. When I_e is negative, the singular point (x_0, x_0) is ESS-stable. (a) The case of the fourth claim in Theorem 4.3 holds and parameters values are as in Fig. 5. (b) The case of the fifth claim in Theorem 4.3 holds and the parameter values are listed in Table 1 except $d_1 = 0.1$, $c_0 = 0.6$, $d_2 = 0.27$, $\sigma_c^2 = 0.009$, $\sigma_a^2 = 0.015$.

Theorem 4.4. *Assume that* $P_T^1 < P_T < P_T^2$. *Let*

$$G_{e2} = \frac{c_0\alpha(\sigma_r^2\sigma_a^2 - \sigma_a^2\sigma_c^2) - d_1\sigma_a^2\sigma_c^2}{a_0(\sigma_r^2\sigma_c^2 - \sigma_a^2\sigma_c^2) + c_0\beta(\sigma_a^2\sigma_c^2 - \sigma_a^2\sigma_r^2)}, \quad {P_T}^{e2} = q_2 G_{e2} + \frac{d_2 q_2}{e a_0}.$$

Then the singular point (x_0, x_0) *is ESS-stable if the one of the following conditions holds*

1. $\dfrac{a_0}{\sigma_a^2} - \dfrac{a_0}{\sigma_r^2} + \dfrac{c_0\beta}{\sigma_r^2} - \dfrac{c_0\beta}{\sigma_c^2} = 0, \ \dfrac{c_0\alpha}{\sigma_c^2} - \dfrac{c_0\alpha}{\sigma_r^2} - \dfrac{d_1}{\sigma_r^2} < 0,$
2. $\dfrac{a_0}{\sigma_a^2} - \dfrac{a_0}{\sigma_r^2} + \dfrac{c_0\beta}{\sigma_r^2} - \dfrac{c_0\beta}{\sigma_c^2} < 0, \ \dfrac{c_0\alpha}{\sigma_c^2} - \dfrac{c_0\alpha}{\sigma_r^2} - \dfrac{d_1}{\sigma_r^2} \leq 0,$

3. $\frac{a_0}{\sigma_a^2}-\frac{a_0}{\sigma_r^2}+\frac{c_0\beta}{\sigma_r^2}-\frac{c_0\beta}{\sigma_c^2}>0$, $\frac{c_0\alpha}{\sigma_c^2}-\frac{c_0\alpha}{\sigma_r^2}-\frac{d_1}{\sigma_r^2}<0$, $P_T^1<{P_T}^{e2}$, $P_T^1<P_T<\max\{{P_T}^{e2},P_T^2\}$,
4. $\frac{a_0}{\sigma_a^2}-\frac{a_0}{\sigma_r^2}+\frac{c_0\beta}{\sigma_r^2}-\frac{c_0\beta}{\sigma_c^2}<0$, $\frac{c_0\alpha}{\sigma_c^2}-\frac{c_0\alpha}{\sigma_r^2}-\frac{d_1}{\sigma_r^2}>0$, $P_T^{e2}<{P_T}^2$, $\max\{{P_T}^{e2},P_T^1\}<P_T<P_T^2$.

Proof. Direct calculations lead to

$$\begin{aligned}\frac{\partial^2 f_1(y_1,x_1,x_2)}{\partial y_1^2} &= [-\frac{1}{\sigma_r^2}+\frac{(y_1-x_0)^2}{\sigma_r^4}]r(y_1)(1-\frac{q_0A^*}{P_T-q_2G^*})\\ &\quad+[\frac{1}{\sigma_c^2}-\frac{(y_1-x_1)^2}{\sigma_c^4}]c(x_1,y_1)A^*+[\frac{1}{\sigma_a^2}-\frac{(y_1-x_2)^2}{\sigma_a^4}]a(y_1,x_2)G^*,\\ \frac{\partial^2 f_2(y_2,x_1,x_2)}{\partial y_2^2} &= [-\frac{1}{\sigma_a^2}+\frac{(y_2-x_1)^2}{\sigma_a^4}]ea(x_1,y_2)A^*.\end{aligned}$$

Since $P_T^1<P_T<P_T^2$, one has $G_0^*=\frac{P_T}{q_2}-\frac{d_2}{\hat{e}a_0}$ and $A_0^*=\alpha-\beta G_0^*$. Then

$$\begin{aligned}\frac{\partial^2 f_1(y_1,x_1,x_2)}{\partial y_1^2}\mid_{y_1=x_1=x_2=x_0} &= (\frac{a_0}{\sigma_a^2}-\frac{a_0}{\sigma_r^2}+\frac{c_0\beta}{\sigma_r^2}-\frac{c_0\beta}{\sigma_c^2})G_0^*+(\frac{c_0\alpha}{\sigma_c^2}-\frac{c_0\alpha}{\sigma_r^2}-\frac{d_1}{\sigma_r^2}),\\ \frac{\partial^2 f_2(y_2,x_1,x_2)}{\partial y_2^2}\mid_{y_2=x_1=x_2=x_0} &= -\frac{ea_0}{\sigma_a^2}A_0^*<0.\end{aligned}$$

When the first or the second claim holds, it is obvious that I_e is always negative and the singular point (x_0,x_0) is always ESS-stable. When the third claim holds, there exists a unique ${P_T}^{e2}$ such that $G_0^*=G_{e2}$. Then $G_0^*<G_{e2}$ for $P_T^2<P_T<{P_T}^{e2}$, and hence $I_e<0$ and the singular point (x_0,x_0) is ESS-stable. If the fourth claim holds, when $P_T>\max\{P_T^2,{P_T}^{e2}\}$, one has $G_0^*>G_{e2}$ and $I_e<0$, whence the singular point (x_0,x_0) is ESS-stable. The proof is complete. □

Theorem 4.4 shows that the singular point $(x_0,x_0)\in X_2$ is always ESS-stable if one of the first two conditions of Theorem 4.3 hold. If the third condition is valid, then the singular point (x_0,x_0) is ESS-stable with lower P_T and is not ESS-stable with higher P_T(Fig. 8(a)). While the singular point (x_0,x_0) is ESS-stable with higher P_T and is not ESS-stable with lower P_T when the fourth condition holds(Fig. 8(b)). From Theorem 4.2 and 4.4, it is not difficult to establish sufficient criteria for the CSS-stability of $(x_0,x_0)\in X_2$ and it follows that the total phosphorus affects the convergence stability and ESS-stability of (x_0,x_0) hence its CSS-stability.

4.2. **Evolutionary branching.** Evolutionary branching occurs when frequency-dependent selection splits a phenotypically monomorphic population into two distinct phenotypic clusters. In this section, based on the discussions above, the evolutionary branching is explored when the singular point (x_0,x_0) is not ESS-stable.

Theorem 4.5. *Assume that* $\sigma_a<\sigma_r$, $P_T>\max\{{P_T}^{b1},P_T^2\}$. *Let*

$$G_{b1}=\frac{\sigma_a^2(c_0d_2+ea_0d_1)}{ea_0^2(\sigma_r^2-\sigma_a^2)},\quad {P_T}^{b1}=q_2G_{b1}+\frac{r_0q_0d_2}{ea_0(r_0-d_1-a_0G_{b1})-c_0d_2}.$$

Then the convergence stable singular point (x_0,x_0) *of* (8) *is an evolutionary branching point.*

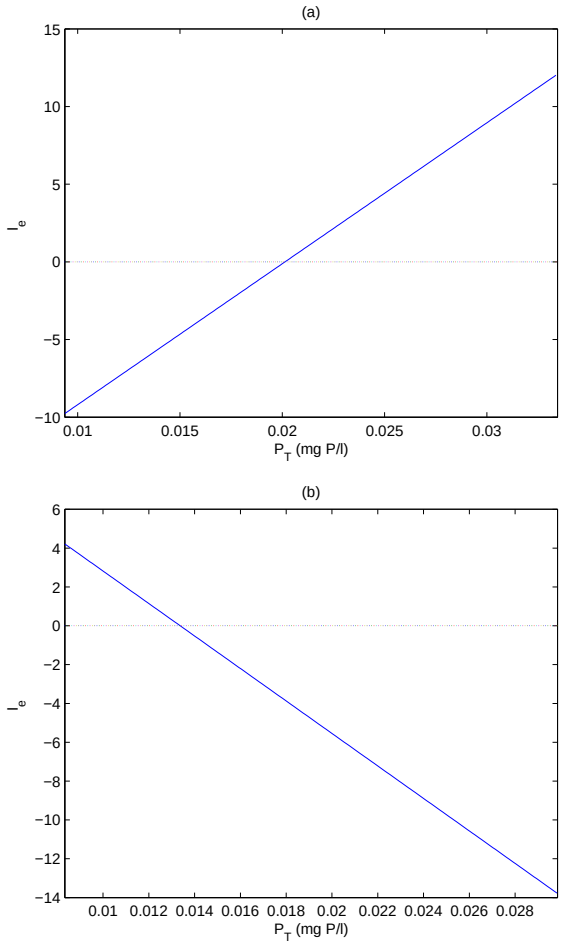

FIGURE 8. The graph of I_e versus P_T with $P_T^1 < P_T < P_T^2$. When I_e is negative, the singular point (x_0, x_0) is ESS-stable. (a) The case of the fourth claim in Theorem 4.4 holds and the parameters values are the same as those in Fig. 5. (b) The case of the fifth claim in Theorem 4.4 holds and the parameter values are listed in Table 1 except $\sigma_c^2 = 0.005$ and $\sigma_a^2 = 0.015$.

Proof. Note that

$$\frac{\partial^2 f_2(y_2, x_1, x_2)}{\partial y_2^2} \mid_{y_2=x_1=x_2=x_0} = -\frac{ea_0}{\sigma_a^2} A_0^* < 0,$$

then $x_2 = x_0$ is always ESS-stable and the evolutionary branching can not happen for the grazer.

For the producer, one has

$$\frac{\partial^2 f_1(y_1, x_1, x_2)}{\partial x_1^2} \mid_{y_1=x_1=x_2=x_0} = -\frac{c_0}{\sigma_c^2} A_0^*,$$
$$\frac{\partial^2 f_1(y_1, x_1, x_2)}{\partial y_1^2} \mid_{y_1=x_1=x_2=x_0} = (\frac{a_0}{\sigma_a^2} - \frac{a_0}{\sigma_r^2}) G_0^* + (\frac{c_0}{\sigma_c^2} - \frac{c_0}{\sigma_r^2}) A_0^* - \frac{d_1}{\sigma_r^2}.$$

Similar to the proof of Theorem 4.1, there exists a unique ${P_T}^{b1}$ such that $G_0^* = G_{b1}$. Then, when $P_T > \max\{{P_T}^{b1}, P_T^2\}$, one has $G_0^* > G_{b1}$, which together with $\sigma_a < \sigma_r$, leads to

$$\frac{\partial^2 f_1(y_1, x_1, x_2)}{\partial x_1^2} \mid_{y_1=x_1=x_2=x_0} > -\frac{\partial^2 f_1(y_1, x_1, x_2)}{\partial y_1^2} \mid_{y_1=x_1=x_2=x_0}.$$

Therefore, the convergence stable singular point (x_0, x_0) is an evolutionary branching point. The proof is complete. □

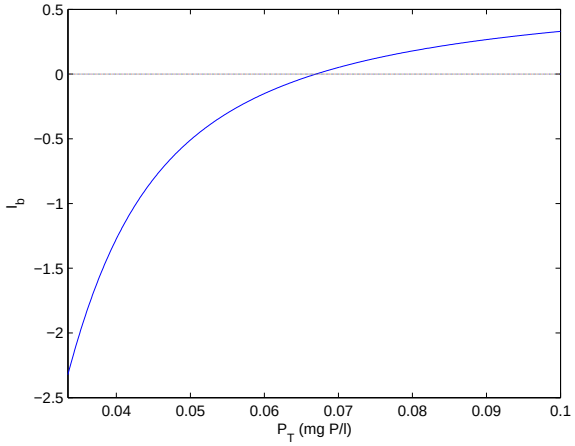

FIGURE 9. The graph of I_b versus P_T with $P_T > P_T^2$. Here $I_b = [\partial f_1^2(y_1, x_1, x_2)/\partial x_1^2 + \partial f_1^2(y_1, x_1, x_2)/\partial y_1^2]|_{y_1=x_1=x_2=x_0}$. The convergence stable singular point (x_0, x_0) is an evolutionary branching point when $I_b > 0$. The parameter values are the same as those in Fig. 5.

If $P_T^2 < {P_T}^{e1}$, then $P_T^2 < {P_T}^{e1} < {P_T}^{b1} < {P_T}^{c1}$ and the singular point $(x_0, x_0) \in X_1$ may be CSS-stable for ${P_T}^2 < P_T < {P_T}^{e1}$, convergence stable but not ESS-stable for ${P_T}^{e1} < P_T < {P_T}^{b1}$, an evolutionary branching point and the producer population becomes dimorphic for ${P_T}^{b1} < P_T < {P_T}^{c1}$. Fig. 9 shows an example that the singular point (x_0, x_0) is an evolutionary branching point for $0.0671 < P_T < 0.2866$. Mutual invasibility plot can help to analyze whether a pair of neighbouring phenotypes on either side of the singular point can invade each other. The set of all pairs of mutually invasible strategies near a singular strategy is given by the overlapping parts of 'shaded' regions in the pairwise invasibility plot [21]. Fig. 10 shows that the mutual invasibility of mutant producer and resident producer is possible when $P_T = 0.1$ and gives rise to a dimorphic producer population.

Theorem 4.6. *Assume that* $\sigma_a < \sigma_r$, $P_T^{b2} < {P_T}^2$, $\max\{{P_T}^{b2}, P_T^1\} < P_T < P_T^2$, *and let*

$$G_{b2} = \frac{c_0\alpha\sigma_a^2\sigma_c^2 + d_1\sigma_a^2\sigma_c^2}{a_0(\sigma_r^2\sigma_c^2 - \sigma_a^2\sigma_c^2) + c_0\beta\sigma_a^2\sigma_r^2}, \quad {P_T}^{b2} = q_2 G_{b2} + \frac{d_2 q_2}{\hat{e}a}.$$

Then the convergence stable singular point (x_0, x_0) *of* (8) *is an evolutionary branching point.*

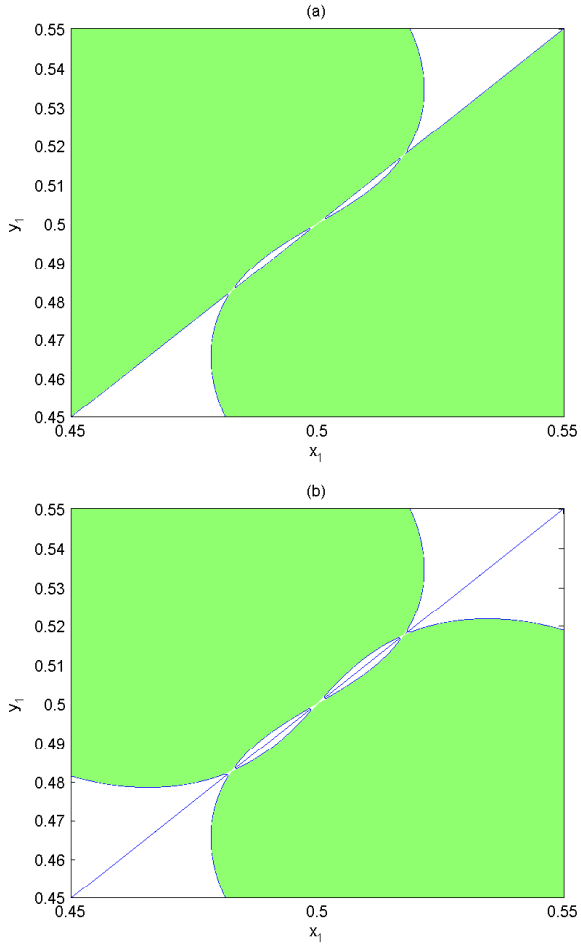

FIGURE 10. (a) Pairwise invasibility plot for fixed grazer trait $x_2 = x_0 = 0.5$. The mutant producer fitness $f_1(y_1, x_1, x_2)$ is positive when (x_1, y_1) is located in the shaded area. The vertical line through x_0 located completely inside the shaded region indicates that the singular point (x_0, x_0) is not ESS-stable. By Theorem 4.5, the singular point (x_0, x_0) is an evolutionary branching point. (b) Mutual invasibility plot for fixed grazer trait $x_2 = x_0 = 0.5$. The second diagonal lies in the shaded region, which shows that the producer population is split into two diverging sub-populations on the long run. The parameter values are the same as those in Fig. 9 except P_T.

Proof. Note that

$$\frac{\partial^2 f_2(y_2, x_1, x_2)}{\partial y_2^2} \mid_{y_2=x_1=x_2=x_0} = -\frac{ea_0}{\sigma_a^2} A_0^* < 0,$$

then $x_2 = x_0$ is always ESS-stable and the evolutionary branching can not happen for the grazer. For the producer, one has

$$\frac{\partial^2 f_1(y_1, x_1, x_2)}{\partial x_1^2} \mid_{y_1=x_1=x_2=x_0} = -\frac{c_0}{\sigma_c^2} A_0^*,$$
$$\frac{\partial^2 f_1(y_1, x_1, x_2)}{\partial y_1^2} \mid_{y_1=x_1=x_2=x_0} = (\frac{a_0}{\sigma_a^2} - \frac{a_0}{\sigma_r^2}) G_0^* + (\frac{c_0}{\sigma_c^2} - \frac{c_0}{\sigma_r^2}) A_0^* - \frac{d_1}{\sigma_r^2}.$$

Similar to the proof of Theorem 4.1, there exists a unique ${P_T}^{b2}$ such that $G_0^* = G_{b2}$. Then, when $\max\{{P_T}^{b2}, P_T^1\} < P_T < P_T^2$, one has $G_0^* > G_{b2}$, which together with $\sigma_a < \sigma_r$, leads to

$$\frac{\partial^2 f_1(y_1, x_1, x_2)}{\partial x_1^2} \mid_{y_1=x_1=x_2=x_0} > -\frac{\partial^2 f_1(y_1, x_1, x_2)}{\partial y_1^2} \mid_{y_1=x_1=x_2=x_0}.$$

Therefore, the convergence stable singular point (x_0, x_0) is an evolutionary branching point. The proof is complete. □

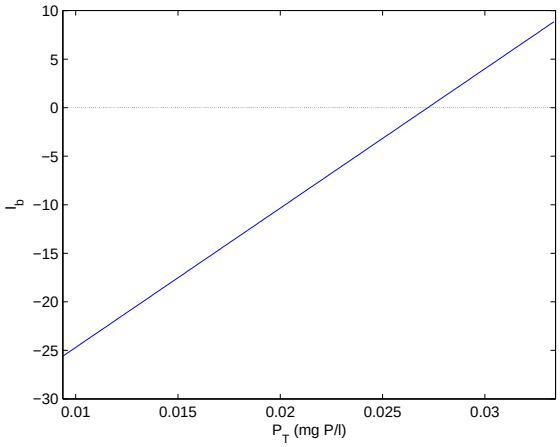

FIGURE 11. The graph of I_b versus P_T with $P_T^1 < P_T < P_T^2$. Here $I_b = [\partial f_1^2(y_1, x_1, x_2)/\partial x_1^2 + \partial f_1^2(y_1, x_1, x_2)/\partial y_1^2]|_{y_1=x_1=x_2=x_0}$. The convergence stable singular point (x_0, x_0) is an evolutionary branching point when $I_b > 0$. The parameter values are listed in Table 1.

If $P_T^1 < {P_T}^{e2} < {P_T}^{b2} < \max\{{P_T}^{c2}, P_T^2\}$, then the singular point $(x_0, x_0) \in X_2$ is CSS-stable for ${P_T}^1 < P_T < {P_T}^{e2}$, is convergence stable but not ESS-stable for ${P_T}^{e2} < P_T < {P_T}^{b2}$, is an evolutionary branching point and the producer population becomes dimorphic for ${P_T}^{b2} < P_T < \max\{{P_T}^{c2}, P_T^2\}$. Fig. 11 shows an example that the singular point (x_0, x_0) is an evolutionary branching point for $0.0272 < P_T < 0.0292$. Fig. 12 shows that the mutual invasibility of mutant producer and resident producer is possible when $P_T = 0.0273$ and gives rise to a dimorphic producer population.

Assume that the two producer branches have equal distance δ on the opposite sides of the singular grazer trait x_0, by carrying out similar arguments to those in

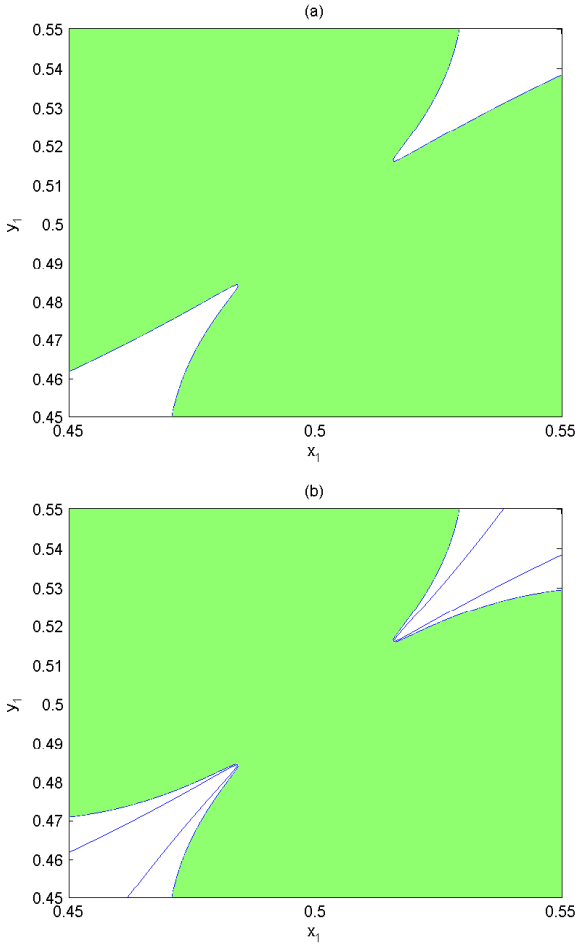

FIGURE 12. (a) Pairwise invasibility plot for fixed grazer trait $x_2 = x_0 = 0.5$. The mutant producer fitness $f_1(y_1, x_1, x_2)$ is positive when (x_1, y_1) is located in the shaded area. The vertical line through x_0 located completely inside the shaded region indicates that the singular point (x_0, x_0) is not ESS-stable. By Theorem 4.5, the singular point (x_0, x_0) is an evolutionary branching point. (b) Mutual invasibility plot for fixed grazer trait $x_2 = x_0 = 0.5$. The second diagonal lies in the shaded region, which shows that the producer population is split into two diverging sub-populations on the long run. The parameter values are listed in Table 1 except P_T.

[13] and [48], one has

$$f_2(y_2, \delta, x_0) = ea(x_0 - \delta, y_2)A/2 + ea(x_0 + \delta, y_2)A/2 - d_2,$$

and

$$\frac{\partial^2 f_2(y_2, \delta, x_0)}{\partial y_2^2} \mid_{y_2 = x_0} = ea_0 A \sigma_a^{-4} \exp\{-\frac{\delta^2}{2\sigma_a^2}\}(\delta^2 - \sigma_a^2),$$

where A is the producer density. If $\delta > \sigma_a$, then

$$\frac{\partial^2 f_2(y_2,\delta,x_0)}{\partial y_2^2}\mid_{y_2=x_0} > 0.$$

Therefore, the mutual invasibility is also possible for grazer near the singular point (x_0, x_0) after the mutual invasibility of producer when two producer branches have moved farther than x_0. The double-invasibility makes the producer-grazer system evolve to an evolutionary branching point and generates four sub-populations (two sub-populations producer and two-subpopulations grazer) on the long run.

4.3. **Evolutionary cycle.** We have studied the CSS-stability and evolutionary branching based on the assumption that the mutants can spread if their fitness is positive and have shown that the population can become dimorphic if the singular point is an evolutionary branching point. Both the CSS-stability and the evolutionary branching require that the singular point has to be convergence stable. In fact, when the singular point is not convergence stable, the traits values may not evolve to the singular point but possibly to a limit cycle. For simplicity, it is assumed that the mutant ones can invade and replace the resident ones only if the mutant ones' fitness is positive to make sure the monomorphism for each population.

Let $x = x_1 - x_0$ and $y = x_2 - x_0$, then (8) becomes

$$\begin{cases} \dfrac{dx}{dt} = m_1[-\dfrac{xR(x)}{\sigma_r^2}(1-\dfrac{q_0A^*}{P_T-q_2G^*}) + \dfrac{(x-y)T(x-y)}{\sigma_a^2}G^*], \\ \dfrac{dy}{dt} = m_2[\dfrac{(x-y)}{\sigma_a^2}eT(x-y)A^*], \end{cases} \tag{13}$$

where

$$\begin{aligned} R(x) &:= r(x+x_0) = r_0\exp\{-\frac{x^2}{2\sigma_r^2}\}, \\ T(x-y) &:= a(x+x_0, y+y_0) = a_0\exp\{-\frac{(x-y)^2}{2\sigma_a^2}\}. \end{aligned}$$

The Jacobian of (13) at (x_1, x_2) reads

$$J(x_1,x_2) = \begin{pmatrix} m_1a_{11} & m_1a_{12} \\ m_2a_{21} & m_2a_{22} \end{pmatrix},$$

where

$$\begin{aligned} a_{11} &= -(\frac{R(x)+xR'(x)}{\sigma_r^2})(1-\frac{q_0A^*}{P_T-q_2G^*}) + [\frac{T(x-y)+(x-y)\partial T(x-y)/\partial x}{\sigma_a^2}]G^*, \\ a_{12} &= [\frac{-T(x-y)+(x-y)\partial T(x-y)/\partial y}{\sigma_a^2}]G^*, \\ a_{21} &= [\frac{T(x-y)+(x-y)\partial T(x-y)/\partial x}{\sigma_a^2}]eA^*, \\ a_{22} &= [\frac{-T(x-y)+(x-y)\partial T(x-y)/\partial y}{\sigma_a^2}]eA^*. \end{aligned}$$

Then the Jacobian of (13) at $(0,0)$ is

$$\begin{aligned} J(0,0) &= \begin{pmatrix} m_1[-\dfrac{r_0}{\sigma_r^2}(1-\dfrac{q_0A_0^*}{P_T-q_2G_0^*}) + \dfrac{a_0}{\sigma_a^2}G_0^*] & -\dfrac{m_1a_0G_0^*}{\sigma_a^2} \\ \dfrac{m_2ea_0A_0^*}{\sigma_a^2} & -\dfrac{m_2ea_0A_0^*}{\sigma_a^2} \end{pmatrix} \\ &= \begin{pmatrix} k-h & -k \\ m & -m \end{pmatrix}, \end{aligned}$$

where

$$k := \frac{m_1 a_0}{\sigma_a^2} G_0^*,\ h := \frac{m_1 r_0}{\sigma_r^2}(1 - \frac{q_0 A_0^*}{P_T - q_2 G_0^*}),\ m := \frac{m_2 e a_0 A_0^*}{\sigma_a^2}.$$

Hence, (13) rewrites

$$\begin{cases} \dfrac{dx}{dt} = (k-h)x - ky + f(x,y), \\ \dfrac{dy}{dt} = mx - my + g(x,y), \end{cases} \tag{14}$$

where

$$f(x,y) = m_1[-\frac{xR(x)}{\sigma_r^2}(1 - \frac{q_0 A_0^*}{P_T - q_2 G_0^*}) + \frac{(x-y)T(x-y)}{\sigma_a^2} G_0^*] + (h-k)x + ky,$$
$$g(x,y) = m_2[\frac{(x-y)}{\sigma_a^2} eT(x-y)A_0^*] - mx + my.$$

Let the Hopf bifurcation conditions be valid [46], i.e., $k - h - m = 0$ and $mh = w^2$, then one has

$$\begin{aligned} \frac{m_1 a_0}{\sigma_a^2} G_0^* &= \frac{m_1 r_0}{\sigma_r^2}(1 - \frac{q_0 A_0^*}{P_T - q_2 G_0^*}) + \frac{m_2 e a_0 A_0^*}{\sigma_a^2}, \\ &= \frac{m_1}{\sigma_r^2}(c_0 A_0^* + d_1 + a_0 G_0^*) + \frac{m_2 e a_0 A_0^*}{\sigma_a^2}. \end{aligned}$$

Note that $k - h - m > 0$ is obviously equivalent to $\mathrm{Tr}(J(x_0, x_0)) > 0$. From the analysis of convergence stability of (x_0, x_0), it follows that, if $\mu_1 \sigma_1^2 \sigma_r^2 > \mu_1 \sigma_1^2 \sigma_a^2 + e\mu_2 \sigma_2^2 \sigma_r^2$ and $P_T^2 < {P_T}^{c1}$, then P_T^{c1} is the Hopf-bifurcation point of (8) for $P_T > P_T^2$. If $\sigma_r^2/\sigma_a^2 > r_0/(r_0 - d_1)$, $(\alpha + \beta\gamma - \delta)^2 - 4\alpha\beta\gamma > 0$, and $P_T^1 < P_T^{c2} < P_T^2 < P_T^{c3}$, then P_T^{c2} is the Hopf-bifurcation point of (8) for $P_T^1 < P_T < P_T^2$. If $\sigma_r^2/\sigma_a^2 > r_0/(r_0 - d_1)$, $(\alpha + \beta\gamma - \delta)^2 - 4\alpha\beta\gamma > 0$, and $P_T^1 < P_T^{c2} < P_T^{c3} < P_T^2$, then P_T^{c2} and P_T^{c3} are the Hopf-bifurcation point of (8) for $P_T^1 < P_T < P_T^2$.

Now we reach the right position to state the Hopf bifurcation claims of (8).

Theorem 4.7. *The following conclusions hold for* (8).

1. *If* $\mu_1 \sigma_1^2 \sigma_r^2 > \mu_1 \sigma_1^2 \sigma_a^2 + e\mu_2 \sigma_2^2 \sigma_r^2$ *and* $P_T^2 < {P_T}^{c1}$, *then a supercritical Hopf bifurcation of* (8) *occurs when* P_T *passes through* P_T^{c1}.
2. *If* $\sigma_r^2/\sigma_a^2 > r_0/(r_0 - d_1)$, $(\alpha+\beta\gamma-\delta)^2 - 4\alpha\beta\gamma > 0$, *and* $P_T^1 < P_T^{c2} < P_T^2 < P_T^{c3}$, *then a supercritical Hopf bifurcation of* (8) *occurs when* P_T *passes through* P_T^{c2}.
3. *If* $\sigma_r^2/\sigma_a^2 > r_0/(r_0 - d_1)$, $(\alpha+\beta\gamma-\delta)^2 - 4\alpha\beta\gamma > 0$, *and* $P_T^1 < P_T^{c2} < P_T^{c3} < P_T^2$, *then a supercritical Hopf bifurcation of* (8) *occurs when* P_T *passes through* P_T^{c2} *and a subcritical Hopf bifurcation of* (8) *occurs when* P_T *passes through* P_T^{c3}.

Fig. 13 plots the bifurcation diagram of (8) against P_T when $P_T > P_T^2$. The singular point $(x_0, x_0) \in X_1$ is convergence stable for $0.0335 < P_T < 0.2866$ and becomes not convergence stable for $P_T > 0.2866$, which suggests that $P_T^{c1} = 0.2866$. When $P_T > P_T^{c1}$, the traits of producer and grazer may possibly oscillate (Fig. 14(b)). The evolutionary dynamics of (8) admit the paradox of nutrient enrichment when $P_T > P_T^2$ (Fig. 14). The evolutionary singular point (x_0, x_0) is convergence stable for P_T being relatively low, and the evolutionary dynamics may evolve to CSS-stability (Fig. 14(a)) or to an evolutionary branching point (Fig. 10). Fig. 15 suggests that the outcome of producer-grazer co-evolution in our model is sensitive to the initial conditions when the total nutrient density in the ecosystem is high. The numerical simulations show that, the evolutionary system (8) possibly admits several different evolution scenarios, e.g., evolving into evolutionary cycle

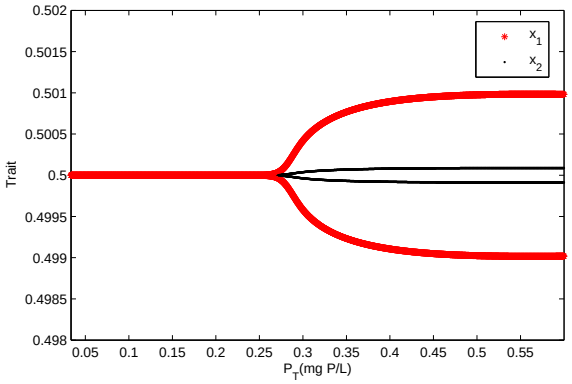

FIGURE 13. A bifurcation diagram of the traits values at the stable state against P_T of (8) for $P_T > P_T^2$. It is observed that $P_T^{c1} \approx 0.2866$ and the producer and grazer coexist cyclically in trait values for $P_T > 0.2866$. The parameters values are the same as those in Fig. 5.

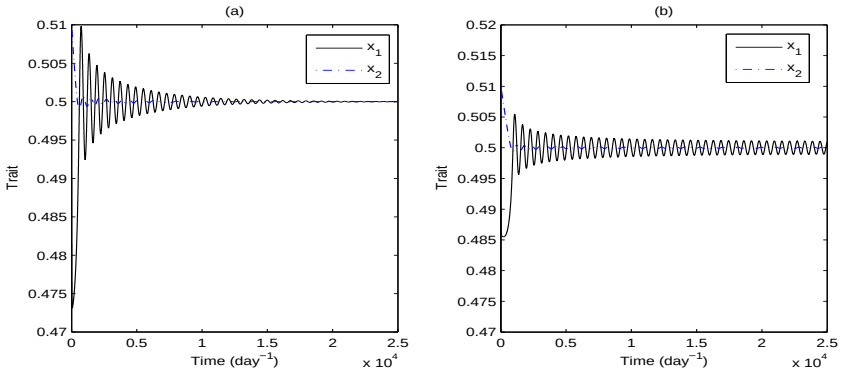

FIGURE 14. The time series of the traits dynamics for $P_T > P_T^2$. (a) The traits of producer and grazer evolve to CSS when $P_T = 0.1$. (b) The traits of producer and grazer evolve to a stable cycle when $P_T = 0.5$. Other parameters values are the same as those in Fig. 5.

(Fig. 15(c)), the traits values keep increasing or decreasing but are still in the coevolution set X (Fig. 15 (a, b, d)).

If $P_T^1 < P_T^{c2} < P_T^2 < P_T^{c3}$, the evolutionary model (8) also admits the paradox of nutrient enrichment(Fig. 16). Fig. 17 depicts the bifurcation diagram of (8) against P_T when $P_T^1 < P_T < P_T^2$. When $0.0094 < P_T < 0.0292$, the singular point $(x_0, x_0) \in X_2$ is convergence stable. When $0.0292 < P_T < 0.0335$, the singular point $(x_0, x_0) \in X_1$ is not convergence stable and evolves into the evolutionary cycle, here $P_T^{c2} = 0.0292$. When $P_T^1 < P_T^{c2} < P_T^{c3} < P_T^2$, the evolutionary model (8) sequently undergoes convergence stability, evolutionary cycle, and convergence stability again with increasing of P_T. Fig. 18 indicates that there are two Hopf bifurcation points $P_T^{c1} = 0.0191$ and $P_T^{c2} = 0.0237$ for $P_T^1 < P_T < P_T^2$. When P_T is approaching to P_T^{c3},

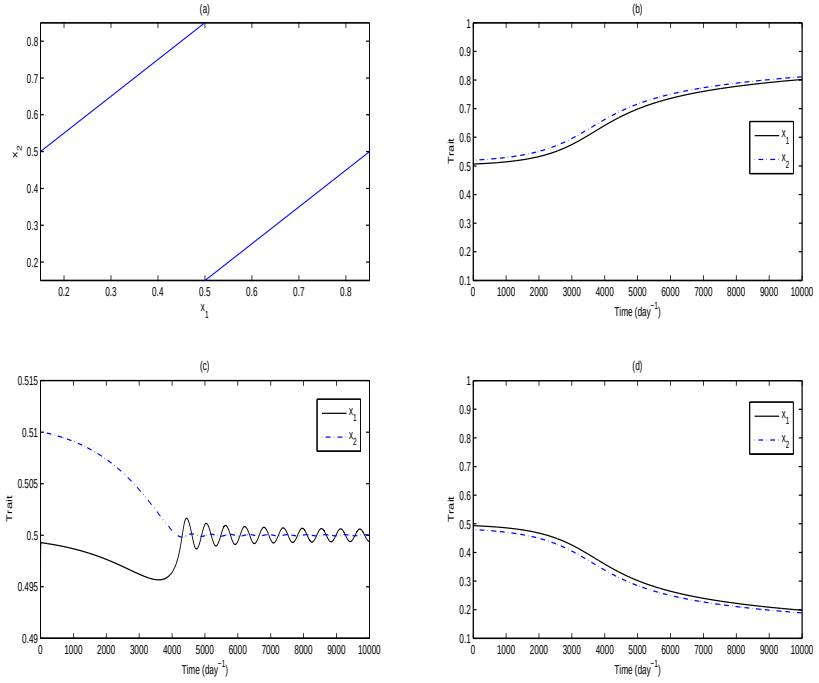

FIGURE 15. The coevolution outcomes are sensitive to the initial conditions under extremely high P_T. (a) The trait set for coevolution with $P_T = 4.6$. (b) The trait values evolve toward large values with $(x_1(0), x_2(0)) = (0.5, 0.52)$. (c) The trait values evolve into an evolutionary cycle with $(x_1(0), x_2(0)) = (0.49, 0.51)$. (d) The trait values evolve toward small values with $(x_1(0), x_2(0)) = (0.49, 0.48)$. The parameter values are the same as those in Fig. 5.

it takes very long time for the evolutionary system to arrive at stable state. So our numerical simulations fail to capture this and the bifurcation curve is discontinuous at P_T^{c3}. In conclusion, qualitative and numerical analyses expound that the total phosphorus plays an important role in the convergence stability of the singular point and also the evolutionary dynamics of (8).

5. **Discussion.** In this paper, we deliberately focus on the effect of nutrient enrichment on the coevolution of the producer-grazer system. An adaptive evolution model is built based on a stoichiometric producer-grazer model (1), which models the impact of the total phosphorus not only on the ecological dynamics but also on the evolutionary dynamics. We systematically carry out detailed qualitative analysis of the evolutionary dynamics of (8). Although the ecological model is very simple, the evolutionary dynamics is rather complex. Our study reveals that total phosphorus asserts a considerable impact on both the ecological dynamics and the evolutionary dynamics.

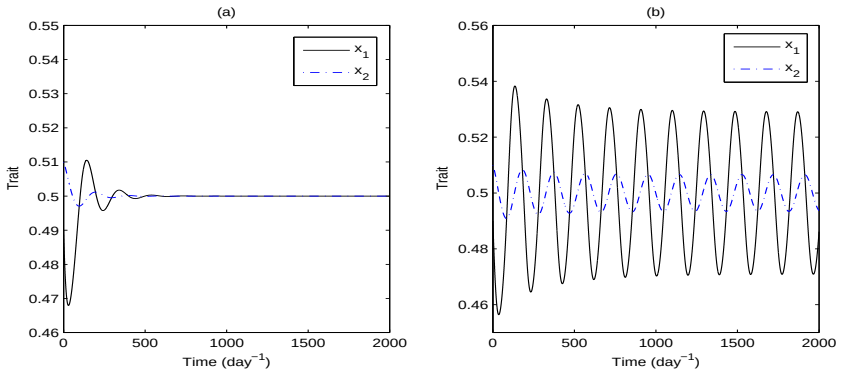

FIGURE 16. The time series of the traits dynamics for $P_T^1 < P_T < P_T^2$ with $P_T^1 < P_T^{c2} < P_T^2 < P_T^{c3}$. (a) The traits of producer and grazer evolve to CSS when $P_T = 0.025$. (b) The traits of producer and grazer evolve to a stable cycle when $P_T = 0.03$. Other parameters values are the same as those in Fig. 6.

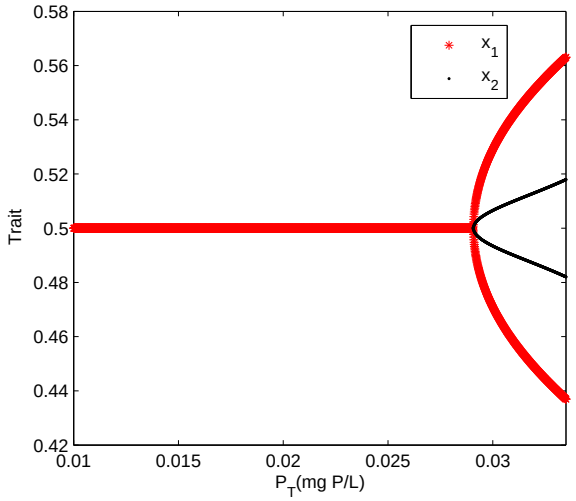

FIGURE 17. A bifurcation diagram of the traits values at the stable state against P_T of (8) for $P_T^1 < P_T < P_T^2$ with $P_T^1 < P_T^{c2} < P_T^2 < P_T^{c3}$. It is observed that $P_T^{c2} \approx 0.0292$ and the producer and grazer coexist cyclically in trait values for $0.0292 < P_T < 0.0335$. The parameters values are the same as those in Fig. 6.

The studies show that the higher total phosphorus is always in favor of the coexistence of producer-grazer system in the ecological dynamics without considering the evolutionary processes. But when the evolutionary process is incorporated, the effects of the total phosphorus are very complicated. When the grazer is absent, lower total phosphorus facilitates the ESS-stability and the CSS-stability, but higher total phosphorus density may produce evolutionary branching and the

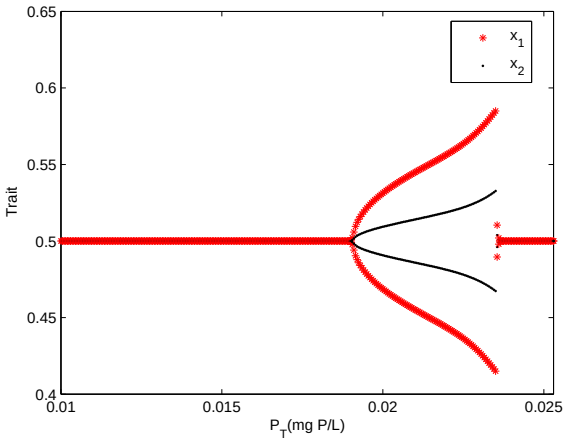

FIGURE 18. A bifurcation diagram of the traits values at the stable state against P_T of (8) for $P_T^1 < P_T < P_T^2$ with $P_T^1 < P_T^{c2} < P_T^{c3} < P_T^2$. It is observed that $P_T^{c1} \approx 0.0191$ and $P_T^{c2} \approx 0.0237$ and the producer and grazer coexist cyclically in trait values for $0.01 < P_T < 0.0253$. The parameters values are the same as those in Fig. 6.

monomorphic population can become distinctively dimorphic. Since the total phosphorus determines the locations of the positive ecological equilibria, the discussion of co-evolution is divided into two cases: $(x_0, x_0) \in X_1$ and $(x_0, x_0) \in X_2$. When $(x_0, x_0) \in X_1$, or $(x_0, x_0) \in X_2$ and $P_T^1 < P_T^{c2} < P_T^2 < P_T^{c3}$, the lower total phosphorus is beneficial to the convergence stability and the singular point is an evolutionary attractor, whereas the higher total phosphorus density can make it an evolutionary repeller and the evolutionary dynamics present oscillations. When $(x_0, x_0) \in X_2$ and $P_T^1 < P_T^{c2} < P_T^{c3} < P_T^2$, the phosphorus enrichment can first destabilize and then stabilize the singular point, which means that (8) subsequently undergoes convergence stability, evolutionary cycle, and convergence stability again. The effect of nutrient enrichment on the ESS-stabilty of the singular point depends on the parameters, and the singular point may be ESS-stable under relatively low total phosphorus or under relatively high total phosphorus. Higher total phosphorus density promotes the evolutionary branching for both $(x_0, x_0) \in X_1$ and $(x_0, x_0) \in X_2$. In summary, increasing the density of total phosphorus may produce complex evolutionary dynamics and trigger the dimorphic populations, a cyclic changes, or sensitive dependence on the initial conditions.

Our model is among the first stoichiometric evolutionary models and sheds some new light on the effect of nutrient on coevolution of the producer and grazer in aquatic ecosystem. It is also more interesting and possibly more challenging to take into account other abiotic or biotic factors such as the global climate changes. In addition, the intrinsic characteristics of target populations may alter the structure and hence enrich the dynamics of the evolutionary model. For example, in our general setting, if the producer represents phytoplankton in lakes, the sinking rate of phytoplankton should be included since it is closely related to the body size of phytoplankton [22]. As in [22], assume that the sinking rate is given by the

well-known Stokes equation $s = \alpha x_1^2$ in the ecological model (5), then the modified evolutionary model reads

$$\begin{cases} \dfrac{dx_1}{dt} = \dfrac{1}{2}\mu_1{\sigma_1}^2 A^*[-\dfrac{(x_1-x_0)r(x_1)}{\sigma_r^2}(1-\dfrac{q_0A^*}{P_T-q_2G^*}) - 2\alpha x_1 \\ \qquad\qquad + \dfrac{(x_1-x_2)a(x_1,x_2)G^*}{\sigma_a^2}], \\ \dfrac{dx_2}{dt} = \dfrac{1}{2}\mu_2{\sigma_2}^2 G^* \dfrac{(x_1-x_2)\hat{e}\min\{1, \dfrac{P_T-q_2G^*}{q_2A^*}\}a(x_1,x_2)A^*}{\sigma_a^2}. \end{cases} \tag{15}$$

One can well investigate its dynamics by carrying out similar arguments as above. Denote the singular point of (15) by (x_1', x_2'). Direct calculations show that $x_1' = x_2'$ and, when $(x_1', x_2') \in X_2'$, $x_1' = x_2'$ is increasing with respect to P_T, here X_2' can be defined in the same way of X_2. It is observed that the body size of producer at the evolutionary equilibrium becomes much larger with the increasing of the total phosphorus when the singular point is convergence stable. This finding supports some existing claims [6, 17, 22] that the phytoplankton communities are dominated by small phytoplankton cells under oligotrophic conditions, whereas larger phytoplankton cells are more abundant when the nutrient concentrations tend to be higher.

Our model expounds the influence of ecological abiotic factors such as nutrient on the coevolution dynamics of producer and grazer by adaptive dynamics, which implies the separation of timescales between ecological and evolution. The past decades also have seen an accumulation of evidences demonstrating that change in ecologically important traits often evolve at the same time and pace as ecological dynamics, which has been observed in diverse species and exploiter-victim systems such as predator-prey interactions [10, 13, 19, 33, 34, 47, 48]. For example, the changes in prey phenotypes can help the prey avoid encounters with predators or defend against attacks, while consumer evolution can allow for increased resource capture and consumption and the ability to overcome prey defense [7]. The eco-evolutionary dynamics describe the interplay between ecological and evolutionary processes with comparable timescales and uncover the reciprocal effects between ecological and evolutionary dynamics. Whence, it is worthy studying the effect of the nutrient enrichment on the stoichiometric eco-evolutionary dynamics.

In our model, in order to clarify the key issues and to facilitate the discussions, the predation rate of the grazer is set to follow a linear Holling's Type I functional response. It prevents nutrient enrichment from yielding predator-prey cycles and ecologically precludes the occurrence of the classical paradox of enrichment [39], which is an important ecological feature that may have a crucial impact on the evolutionary dynamics of the model. More recent theoretical works have demonstrated that a particular mathematical form of functional response has surprising effects on the ecological dynamics of the predator-prey interactions. So, it is more interesting but more challenging to consider more realistic formulations which incorporate the functional response of different types such as prey-dependent or predator-dependent and check the similarities or key difference of the evolutionary dynamics. In addition, (15) assumes that phosphorus in the sinking phytoplankton is immediately released back while, in reality, some of such phosphorus stays on the bottom of lakes and then the total phophorus in the system is reduced. Therefore, the sinking process needs a more thoughtful modeling approach. Those topics are left to our future work.

Acknowledgments. The authors would like to thank Dr. Irakli Loladze for his excellent comments and suggestions, which greatly improve the presentation of the paper.

REFERENCES

[1] P. A. Abrams and J. D. Roth, The effects of enrichment of three-species food chains with nonlinear functional response, *Ecology,* **75** (1994), 1118–1130.
[2] A. N. Mizuno and M. Kawata, The effects of the evolution of stoichiometry-related traits on population dynamics in plankton communities, *J. Theor. Biol.,* **259** (2009), 209–218.
[3] D. M. Anderson, P. M. Glibert and J. M. Burkholder, Harmful algal blooms and eutrophication: Nutrient sources, composition, and consequences, *Estuaties,* **25** (2002), 704–726.
[4] A. Binzer, C. Guill, U. Brose and B. C. Rall, The dynamics of food chains under climate change and nutrient enrichment, *Phil. Trans. R. Soc. B,* **367** (2012), 2935–2944.
[5] P. Branco, M. Stomp, M. Egas and J. Huisman, Evolution of nutrient uptake reveals a trade-off in the ecological stoichiometry of plant-herbivore interactions. *Am. Nat.,* **176** (2010), 162–176.
[6] S. Chisholm, Phytoplankton size, In *Primary Productivity and Biogeochemical Cycles in the Sea*, **43** (1992), 213–237.
[7] M. Cortez and S. P. Ellner, Understanding rapid evolution in predator-prey interactions using the theory of fast-slow dynamical systems, *Am. Nat.,* **176** (2010), E109–E127.
[8] J. M. Davis, A. D. Rosemond, S. L. Eggert, W. F. Cross and J. B. Wallace, Long-term nutrient enrichment decouples predator and prey production, *Proc. Natl. Acad. Sci. USA,* **107** (2010), 121–126.
[9] U. Dieckmann and R. Law, The dynamical theory of coevolution: A derivation from stochastic ecological processes, *J. Math. Biol.,* **34** (1996), 579–612.
[10] U. Dieckmann, P. Marrow and R. Law, Evolutionary cycling in predator-prey interactions: Population dynamics and the red queen, *J. Theor. Biol.,* **176** (1995), 91–102.
[11] S. Diehl, Paradoxes of enrichment: Effects of increased light versus nutrient supply on pelagic producer-grazer system, *Am. Nat.,* **169** (2007), 173–191.
[12] S. Diehl and M. Feißel, Effects of enrichment on three-level food chainswith omnivory, *Am. Nat.,* **155** (2000), 200–218.
[13] M. Doebeli and U. Dieckmann, Evolutionary branching and sympatric speciation caused by different types of ecological interactions, *Am. Nat.,* **156** (2000), S77–S101.
[14] M. R. Droop, Vitamin b_{12} and marine ecology. iv. the kinetics of uptake, growth and inhibition in monochrysis lutheri, *J. Mar. Biol. Assoc. UK,* **48** (1968), 689–733.
[15] T. H. G. Ezard, S. D. Côté and F. Pelletier, Eco-evolutionary dynamics: Disentangling phenotypic, environmental and population fluctuations, *Phil. Trans. R. Soc. B,* **364** (2009), 1491–1498.
[16] Z. V. Finkel, M. E. Katz, J. D. Wright, O. M. E Schofield and P. G. Falkowski, Climatically driven macroevolutionary patterns in the size of marine diatoms over the cenozoic, *Proc. Natl. Acad. Sci. USA,* **102** (2005), 8927–8932.
[17] Z. V. Finkel, J. Beardall, K. J. Flynn, A. Quigg, T. A. Rees and J. Raven, Phytoplankton in a changing world: Cell size and elemental stoichiometry, *J. Plankton. Res.,* **32** (2010), 119–137.
[18] G. F. Fussmann, S. P. Ellner and N. G. Hairston, Evolution as a critical component of plankton dynamics, *Proc. R. Soc. Lond. B,* **270** (2003), 1015–1022.
[19] G. F. Fussmann, M. Loreau and P. A. Abrams, Eco-evolutionary dynamics of communities and ecosystems, *Funct. Ecol.,* **21** (2007), 465–477.
[20] S. A. H. Geritz and M. Gyllenberg, Seven answers from adaptive dynamics, *J. EVOL. BIOL.,* **18** (2005), 1174–1177.
[21] S. A. H. Geritz, E. Kisdi, G. Meszéna and J. A. J. Metz, Evolutionarily singular strategies and the adaptive growth and branching of the evolutionary tree, *Evol. Ecol.,* **12** (1998), 35–57.
[22] L. Jiang, O. M. E. Schofield and P. G. Falkowski, Adaptive evolution of phytoplankton cell size, *Am. Nat.,* **166** (2005), 496–505.
[23] M. D. John, A. D. Rosemond, S. L. Eggert, W. F. Cross and J. B. Wallace, Nutrient enrichment differentially affects body sizes of primary consumers and predators in a detritus-based stream, *Limnol. Oceanogr.,* **55** (2010), 2305–2316.

[24] L. E. Jones, L. Becks, S. P. Ellner, N. G. Hairston, T. Yoshida and G. F. Fussmann, Rapid contemporary evolution and clonal food web dynamics, *Phil. Trans. R. Soc. B,* **364** (2009), 1579–1591.
[25] E. Kisdi, Evolutionary branching under asymmetric competition, *J. Theor. Biol.,* **197** (1999), 149–162.
[26] C. A. Klausmeier, E. Litchman and S. A. Levin, A model of flexible uptake of two essential resources, *J. Theor. Biol.,* **246** (2007), 278–289.
[27] X. Li, H. Wang and Y. Kuang, Global analysis of a stoichiometric producer-grazer model with Holling type functional responses, *J. Math. Biol.,* **63** (2011), 901–932.
[28] N. Loeuille and M. Loreau, Nutrient enrichment and food chains: Can evolution buffer top-down control? *Theor. Popul. Biol.,* **65** (2004), 285–298.
[29] N. Loeuille and M. Loreau, Evolutionary emergence of size-structured food webs, *Proc. Natl. Acad. Sci. USA,* **102** (2005), 5761–5766.
[30] N. Loeuille, M. Loreau and R. Ferrière, Consequences of plant-herbivore coevolution on the dynamics and functioning of ecosystems, *J. Theor. Biol.,* **217** (2002), 369–381.
[31] I. Loladze, Y. Kuang and J. J. Elser, Stoichiometry in producer-grazer systems: Linking energy flow and element cycling, *Bull. Math. Biol.,* **62** (2000), 1137–1162.
[32] M. Loreau, Ecosystem development explained by competition within and between material cycles, *Proc. R. Soc. Lond. B,* **265** (1998), 33–38.
[33] A. Mougi and Y. Iwasa, Evolution towards oscillation or stability in a predator-prey system, *Proc. R. Soc. B,* **277** (2010), 3163–3171.
[34] A. Mougi and Y. Iwasa, Unique coevolutionary dynamics in a predator-prey system, *J. Theor. Biol.,* **277** (2011), 83–89.
[35] E. B. Muller, R. M. Nisbet, S. A. L. M Kooijman, J. J. Elser and E. McCauley, Stoichiometric food quality and herbivore dynamics, *Ecol. Lett.,* **4** (2001), 519–529.
[36] D. Pimentel, Animal population regulation by the genetic feed-back mechanism, *Am. Nat.,* **95** (1961), 65–79.
[37] J. A. Raven, Physiological consequences of extremely small size for autotrophic organisms on the sea, *Can. Bull. Fish. Aquat. Sci.,* **214** (1986), 1–70.
[38] J. A. Raven, Why are there no picoplanktonic o_2 evolvers with volumes less than $10^{-19}m^3$? *J. Plankton. Res.,* **16** (1994), 565–580.
[39] M. L. Rosenzweig, Paradox of enrichment: Destabilization of exploitation ecosystems in ecological time, *Science,* **171** (1971), 385–387.
[40] R. W. Sterner and J. J. Elser, *Ecological Stoichiometry: The Biology of Elements from Molecules to the Biosphere,* NJ: Princeton University Press, Princeton, 2002.
[41] D. Stiefs, G. A. K. Van Voorn, B. W. Kooi, U. Feudel and T. Gross, Food quality in producer-grazer models-: A generalized analysis, *Am. Nat.,* **176** (2010), 367–380.
[42] A. Verdy, M. Follows and G. Flierl, Optimal phytoplankton cell size in an allometric model, *Mar. Ecol. Prog. Ser.,* **379** (2009), 1–12.
[43] H. Wang, H. L. Smith, Y. Kuang and J. J. Elser, Dynamics of stoichiometric bacteria-algae interaction in epilimnion, *SIAM J. Appl. Math.,* **68** (2007), 503–522.
[44] D. Waxman and S. Gavrilets, 20 questions on adaptive dynamics, *J. Evol. Biol.,* **18** (2005), 1139–1154.
[45] T. G. Whitham, J. K. Bailey and J. A. Schweitzer et al, A framework for community and ecosystem genetics: From genes to ecosystems, *Nature Reviews Genetics,* **7** (2006), 510–523.
[46] S. Wiggins, *Introduction to Applied Nonlinear Dynamical Systems and Chaos*, Springer-Verlag, New York, 1990.
[47] T. Yoshida, L. E. Jones, S. P. Ellner, G. F. Fussmann and Jr N. G. Hairston, Rapid evolution drives ecological dynamics in a predator-prey system, *Nature,* **424** (2003), 303–306.
[48] J. Zu, M. Mimura and J. Y. Wakano, The evolution of phenotypic traits in a predator-prey system subject to Allee effect, *J. Theor. Biol.,* **262** (2010), 528–543.

Received September 18, 2013; Accepted December 18, 2013.

E-mail address: haoln500@nenu.edu.cn
E-mail address: mfan@nenu.edu.cn
E-mail address: wangx902@nenu.edu.cn